Brain-inspired computing with self-assembled networks of nano-objects

Journal of Physics D: Applied Physics

PURPOSE-LED PUBLISHING™

TOPICAL REVIEW • OPEN ACCESS

Brain-inspired computing with self-assembled networks of nano-objects

To cite this article: Alexander Vahl *et al* 2024 *J. Phys. D: Appl. Phys.* **57** 503001

OPEN ACCESS
IOP Publishing

Journal of Physics D: Applied Physics

J. Phys. D: Appl. Phys. 57 (2024) 503001 (24pp)

https://doi.org/10.1088/1361-6463/ad7a82

Topical Review

Brain-inspired computing with self-assembled networks of nano-objects

Alexander Vahl[1,2], **Gianluca Milano**[3], **Zdenka Kuncic**[4], **Simon A Brown**[5] **and Paolo Milani**[6,*]

[1] Chair for Multicomponent Materials, Department of Materials Science, Faculty of Engineering, Kiel University, Kaiserstraße 2, D-24143 Kiel, Germany
[2] Leibniz Institute for Plasma Science and Technology, Felix-Hausdorff-Str. 2, 17489 Greifswald, Germany
[3] Advanced Materials Metrology and Life Sciences Division, INRiM (Istituto Nazionale di Ricerca Metrologica), Strada delle Cacce 91, 10135 Torino, Italy
[4] School of Physics and Sydney Nano Institute, University of Sydney, Sydney, NSW 2006, Australia
[5] The MacDiarmid Institute for Advanced Materials and Nanotechnology School of Physical and Chemical Sciences, Te Kura Matu, University of Canterbury, Christchurch 8140, New Zealand
[6] CIMAINA (Centro Interdisciplinare Materiali e Interfacce Nanostrutturati), Dipartimento di Fisica 'A. Pontremoli', Università degli Studi di Milano, via Celoria 16, 20133 Milano, Italy

E-mail: paolo.milani@mi.infn.it

Received 21 April 2024, revised 28 August 2024
Accepted for publication 13 September 2024
Published 26 September 2024

Abstract

Major efforts to reproduce functionalities and energy efficiency of the brain have been focused on the development of artificial neuromorphic systems based on crossbar arrays of memristive devices fabricated by top-down lithographic technologies. Although very powerful, this approach does not emulate the topology and the emergent behavior of biological neuronal circuits, where the principle of self-organization regulates both structure and function. In materia computing has been proposed as an alternative exploiting the complexity and collective phenomena originating from various classes of physical substrates composed of a large number of non-linear nanoscale junctions. Systems obtained by the self-assembling of nano-objects like nanoparticles and nanowires show spatio-temporal correlations in their electrical activity and functional synaptic connectivity with nonlinear dynamics. The development of design-less networks offers powerful brain-inspired computing capabilities and the possibility of investigating critical dynamics in complex adaptive systems. Here we review and discuss the relevant aspects concerning the fabrication, characterization, modeling, and implementation of networks of nanostructures for data processing and computing applications. Different nanoscale electrical conduction mechanisms and their influence on the meso- and macroscopic functional

* Author to whom any correspondence should be addressed.

properties of the systems are considered. Criticality, avalanche effects, edge-of-chaos, emergent behavior, synaptic functionalities are discussed in detail together with applications for unconventional computing. Finally, we discuss the challenges related to the integration of nanostructured networks and with standard microelectronics architectures.

Keywords: self-assembled, networks, nano-objects, neuromorphic

1. Introduction

Neuromorphic computing relies on the use of electronic devices to mimic the organization and the performance of mammalian nervous systems [1]. Key aspects to be reproduced in order to perform complex tasks with a reduced energy consumption, are learning and development, adaptation to local changes (plasticity), event-driven signaling, robustness to damage, and in-memory information processing [1]. To this purpose, considerable efforts are directed to the fabrication of devices reproducing the behavior of elemental biological building blocks such as neurons and synapses in order to assemble them and to create 'brain-inspired' structures [2]. The core of this vision is to exploit neuroscience-driven concepts to realize brain-inspired systems able to emulate some features of how information is processed in our brain [3].

In 1940 Shannon *et al* demonstrated, in his master thesis, that a small set of electrical components could be assembled to compute the result of any compound Boolean logic operation [4]. Almost ten years later, in a lecture given at Caltech, von Neumann stated '[…] logical propositions can be represented as electrical networks or (idealized) nervous systems. Whereas logical propositions are built-up by combining certain primitive symbols, networks are formed by connecting basic components, such as relays in electrical circuits and neurons in the nervous system' [5].

An alternative point of view to this deterministic approach, was proposed by Block *et al* with the 'perceptron' considered as a probabilistic model for information storage and organization in the brain [6]. Unfortunately, the complexity of Rosenblatt's model was not immediately recognized and the perceptron was considered as a simple on-off electronic component capable of performing classification tasks only for linearly separable Boolean functions [7]. The advent of artificial neural networks (ANNs) prompted the reconsideration of the perceptron as the simplest ANN unit specifically able to implement an adjustable logic operation through the calibration of 'synaptic weights' [8–11]. A single perceptron can be used to generate linearly separable Boolean functions, while more complex mappings can be achieved via multilayer perceptrons [12].

Currently, devices used as building blocks for neuromorphic systems, including non-volatile memory devices, are fabricated by top-down lithographic methods typical of highly integrated CMOS component found in traditional computer architectures [13]. While this is considered an effective solution for many applications, unconventional bottom-up fabrication approaches have been proposed and are actively investigated [1, 14–16]. The aim is to go beyond solutions based on the Turing paradigm [17] by using hardware and physical architectures relying on emergent complexity and collective phenomena originating from various classes of physical substrates [18–21]. These methods are especially promising for classifying complex data through the nonlinear projection into high-dimensional spaces with a computational cost significantly lower compared to that of methods running on von Neuman computers. Examples of such approaches include quantum computing, optical computing, chemical computing, and in materia computing.

In the last decade, networks consisting of a large number of non-linear nanoscale junctions have been considered [18]: in these systems, obtained by the self-assembling of nanostructures like nanoparticles and nanowires [22, 23], the 'deterministic' structure of microelectronic circuits is replaced by the complex connectivity of nanostructures with non-linear conduction properties characterized by spatiotemporal correlation in the electrical activity, in analogy with the brain [20, 24, 25]. This behavior emerges from the presence of high density of non-linear and recurrent junctions formed at the nanoscale during the synthesis process. Examples of such networks are those based on atomic switches, nanoparticles, or nanowires [23, 26]; in particular nanowire networks have shown long-term connectivity retention [22], hierarchical collective dynamics [24], and heterosynaptic plasticity [18]. Long range temporal correlations [27] and criticality [20, 28] have been reported in nanoparticle networks.

One of the earliest studies to report collective brain-like dynamics emerging from self-organized nano-structured networks was that of Stieg *et al* [29], who observed stochastic bursts and fluctuations with power–law scaling in the conductivity of Ag_2S nanowire networks (referred to as atomic switch networks following previous work on synaptic Ag_2S atomic switch single memristor devices [30]). These dynamics are qualitatively similar in nature to the transient and stochastic oscillatory coherence that is thought to underlie flexible information routing in the brain [31]. This early work inspired much of the subsequent work on nanoparticle and nanowire networks.

Here we review and discuss the relevant aspects concerning the fabrication, characterization, modeling and implementation of nanostructured networks for computing and data processing applications. Different nanoscale electrical conduction mechanisms and their influence on the meso- and macroscopic functional properties of the systems are considered. Criticality, avalanche effects, edge-of-chaos, emergent behavior, synaptic functionalities are discussed in detail together with applications for unconventional computing. Finally, we discuss the challenges related to the integration of nanostructured networks with standard microelectronics architectures.

2. Fabrication of self-organizing nanoarchitectures

The successful evolution of microelectronic technologies based on the CMOS paradigm is based on the exponential increase of device density [32]. The trend of this continuous downscaling cannot continue at the same pace due to the complexity of device cross-sections at nanometer scale. In particular, power dissipation issues, wire architectures and the need of low threshold voltages represent serious issues. The top-down fabrication of complex and highly packed nanoscale circuits requires the use of extremely expensive lithographic techniques in term of investments and running costs [33].

Bottom-up self-assembly techniques have been proposed as a possible alternative for the realization of complex 2D and 3D structures using nano-objects as building blocks [33]. This approach is extremely affordable from the economic point of view compared to lithographic techniques and it can produce networks characterized by a multiscale complexity that is a pivotal trait in biological neural systems [16].

2.1. Bottom-up approach: self-assembly and self-organization of nanoscopic building units

In bottom-up approaches, extended networks or assemblies of self-similar building units are formed, either by self-assembly or self-organization, making use of internal (e.g. interfacial energies) and external (e.g. potential gradients) driving forces, respectively. Self-assembly and self-organization determine the arrangement of the preformed building units, which are commonly molecules or objects with nanoscopic dimensions such as nanosheets (2D objects), nanowires (1D objects) or nanoparticles (0D objects). While bottom-up approaches commonly do not enable an external control over the exact positioning of each individual component, self-assembly and self-organization are employed to achieve control over the components' connectivity to yield a given target integrated layout and functionality. Preformed clusters, nanoparticles, and nanowires produced by wet chemistry or physical methods can be deposited on a substrate with varying degree of coverage, ranging from sparse, diluted systems to continuous nanostructured layers. In this framework different nanoscale conduction mechanisms can be exploited for the realization of complex nanoscale networks where the information processing capability arise from the interplay in between structure and function similarly to biological neural systems [34].

With most resistive switching (RS) phenomena being crucially linked to the nanoscale, devices based on nanostructures, including nanocrystals, nanoparticles, or nanowires per se can exhibit a large range of RS features. A particular interest in the use of nanoobjects compared to atom-assembled thin films lies in the potential to decrease current levels, to localize electric fields and to confine locations for memristive switching processes. Due to the nanoscale dimensions and the variance in the exact placement due to the chosen bottom-up synthesis techniques, in many cases it is not possible to directly address individual nanoobjects for electrical characterization via conventional means (i.e. pre-structured, planar electrodes). Therefore, in large-scale networks of nanoobjects, RS is mostly studied as a collective response. To understand RS at the level of individual nanoobjects, analytic approaches with precise local contacting, in particular conductive atomic force microscopy (c-AFM), is commonly applied. Examples for local investigations on individual nanoobjects include studies on RS in nanorods, nanoparticles and nanowires [35–37].

In this review, we focus on recent trends in vacuum- and liquid-based methods, both for the formation of nanoobjects as building units, as well as for the deposition and assembly and organization towards nanogranular networks. Beyond the scope are further applications of bottom-up approaches such as creating nanostructured electrodes and matrices that are capable of localizing contact areas and confining RS processes, e.g. by using self-assembled PbS quantum dots on an inert Pt electrode, or self-assembled SiO_x nanoparticle arrays, guiding metal filament growth [38–40].

2.2. Vacuum-based methods

The synthesis of nanostructured systems based on the random assembling of nanoparticles by physical methods relies on gas-phase techniques [41] (figure 1(a)). In gas phase synthesis, nanoparticles are made by 'building' them from individual atoms or molecules up to the desired size: nuclei are formed either by physical means such as condensation of a supersaturated vapor or by chemical reaction of gaseous precursors [41]; subsequent to the formation of solid particles is the deposition on a substrate.

Vacuum processes for solid particle deposition usually rely on expansion techniques that pass particles in a gas through an orifice or nozzle, after which expansion takes place to give a beam of particles that can be deposited onto a surface [46]. The starting vapor can be generated by a variety of means such as Joule heating of a material in a crucible, laser ablation, sputtering, or arc discharge (figure 1(a)).

Compact nanostructured films can be produced by the assembling of preformed nanoparticles (clusters) in the gas phase and, in particular by cluster beam deposition (CBD) [47–49]. A systematic characterization of the growth process of nanostructured films produced by CBD from submonolayer to thickness of hundreds of nanometers can be found in [50–52]. The process of film formation takes place in a ballistic deposition regime [50], consequently, the deposition time is the main parameter that allows for the control of the film surface morphology that evolves regularly according to simple and reproducible scaling laws [51] (figures 1(c) and (d)).

Supersonic cluster beam deposition (SCBD) has been demonstrated as an effective approach for the synthesis of cluster-assembled nanostructured systems showing neuromorphic behavior [53]. SCBD is characterized by a high deposition rate, high lateral resolution (compatible with planar microfabrication technologies) and neutral particle mass

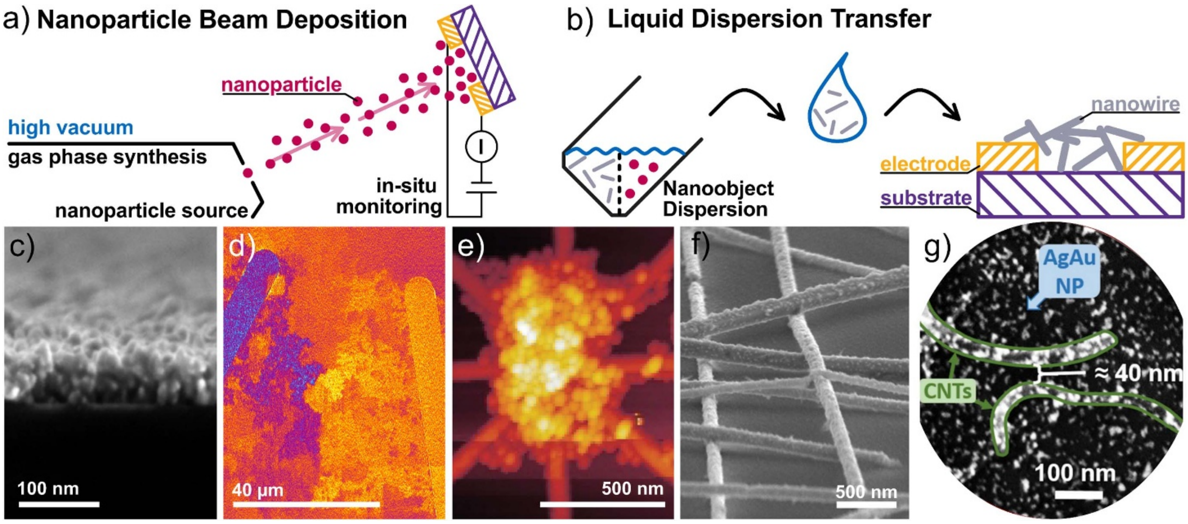

Figure 1. Bottom-up methods for nanogranular networks include vapor phase methods (a) as well as solution processing (b). Examples for self-organized nanogranular networks: (c) side view of a percolated Au nanoparticle network deposited by SCBD; (d) Ag-based nanoparticle network at the percolation threshold in resistive contrast imaging [42] (top view). [42] John Wiley & Sons. [Copyright © 2024 WILEY-VCH Verlag GmbH & Co. KGaA, Weinheim]; (e) network of Au nanoparticles with a 1-octanethiol SAM (top view, including electrode array) [43]. Reproduced from [43], with permission from Springer Nature; (f) self-organized arrangement of Ag nanowires in a quasi-2D network [44]. Reproduced from [44]. CC BY 4.0; (g) nanogranular network with CNTs and sparse AgAu nanoparticle coverage [45]. Reproduced from [45]. CC BY 4.0.

selection process by exploiting aerodynamic focusing effects [54]. SCBD is an enabling tool for the large-scale integration of nanoparticles and nanostructured films on microfabricated platforms and smart nanocomposites [55]. A source particularly suited for the production of intense and stable neutral supersonic cluster beams is the pulsed microplasma cluster source, as described in details in [56, 57]. High directionality, collimation and intensity of aerodynamically focused supersonic cluster beams, make them well suited for patterned deposition of nanostructured films through non-contact stencil masks or lift-off technologies [58, 59].

In a similar approach, in a gas aggregation source (GAS), a super-saturated vapor is formed by magnetron sputtering. This method was found to be useful for fabrication of memristive networks of nanoparticles [60, 61] and is particularly interesting for the gas phase synthesis of alloy nanoparticles, e.g. AgAu and AgPt, with the potential to monitor and control the nanoparticle composition in-operando [62, 63]. Commonly, a GAS is operated via a continuous DC plasma discharge and under a constant pressure gradient between source and main vacuum system, which facilitates the deposition of (memristive) nanocomposites via embedding particles into a dielectric matrix, using secondary vacuum-based deposition techniques [28, 36, 37]. As found for most CBD techniques, GAS is compatible with a large range of substrates, enabling the modification of preformed nanoobject networks (e.g. sparse carbon nanotube (CNT) networks) and even the direct deposition of nanoparticles into liquid media [45, 64].

The efficient decoupling of cluster (or nanoparticle) production, manipulation and deposition in a typical CBD apparatus allows the *in-situ* characterization of the evolution of the electrical properties of cluster-assembled films during the fabrication process.

2.3. Liquid-based methods

Liquid-based methods typically involve a dispersion of the nanoobjects in a host liquid, that is used to transfer them to a suitable substrate, where the host liquid is removed (e.g. via evaporation) and leaves behind a network of nanoobjects (figure 1(b)). Controlling the agglomeration of individual nanoobjects, for example by the means of external control parameters such as a locally applied electrical field, can be used as a viable route to tailor the connectivity within the resulting nanogranular network. A certain degree of control over the connectivity can be obtained by tailoring the concentration of nanoobjects in the dispersion and via the applied deposition process (i.e. spin coating, dip coating or drop casting). By embedding nanoparticles, e.g. Ag, from gas phase synthesis using a gas directly into liquid host media under constant stirring it is possible to obtain dispersions without the use of surfactants. Here, long range conductive pathways could be dynamically reconfigured due to self-organization of Ag nanoparticles in an applied electrical field [64]. However, typically, nanogranular networks that are obtained from liquid-based methods do not rely on pure metal nanoobjects, but apply surfactants, SAMs or polymer capping. For example, dielectrophoresis has been applied to create self-organized compact nanoparticle networks, e.g. by Bose *et al* using a dispersion of Au nanoparticles (with 20 nm diameter) and a SAM of 1-octanethiol in a mixture of ethanol and polyethylene glycol (figure 1(e)) [43]. Further approaches also extend to non-metallic nanoparticles, such as functionalized $SrTiO_3$ with a SAM of oleic acid, aligned to nanoribbons [65] or mixed nanoparticle networks, e.g. of $BaZrO_3$ and $SrZrO_3$, functionalized by 2-hexadecylphosphonic acid. Combining two types of preformed nanoobjects, the size distribution and size difference between each species of nanoobject strongly determines the overall connectivity between the building units and thus is an additional control parameter to influence the electrical properties of the network [66].

Self-assembled neuromorphic NW networks have been realized mainly through drop casting, spray deposition or electroless deposition. In case of drop-casting, the fabrication of NW networks occurs through the dispersion of core–shell NWs in solution on a substrate [18, 24], realizing a highly interconnected network of randomly dispersed NWs as reported in figure 1(f). This represents a low-cost fabrication technique that does not require nanolithography steps and cleanroom facilities. To realize neuromorphic networks, usually either metal–oxide NWs or core–shell NWs with an Ag inner core and a polymeric (such as a poly(vinylpyrrolidone), PVP) shell have been exploited to form metal–insulator–metal memristive junctions at the NW–NW intersection [67]. As an alternative to drop-casting, spray deposition can be exploited to deposit NWs in a solution on an insulating substrate [23, 68]. Instead, a different approach is represented by electroless deposition, where self-assembled NW networks are realized by coupling conventional top-down CMOS photolithography with bottom-up self-assembly through chemical processes [26, 30, 69]. Complex NW structures have been grown from nano-patterned metallic seeds to form networks of intersecting metallic Ag NWs. A subsequent sulfurization process is exploited to realize Ag–Ag_2S–Ag metal–insulator–metal junctions at NW intersections that act RS cells, usually referred as 'Atomic Switch Networks'. Nanoparticle assemblies have also been combined with one-dimensionally extended nanoobjects, such as CNTs, e.g. to obtain lateral sparse arrays with RS features (figure 1(g)) [45].

3. Nanoscale physics for computing

Memristive devices and memristive-based architectures showing RS represent a paradigm for a large number of approaches proposed for unconventional computing. [70–73] Among the various RS physical mechanisms that have been exploited, redox-based memristive devices—nanoscale electrochemical systems where ionics is coupled with electronics—is prominent [15]. Of particular importance is the fact that device functionalities are related to atomic reconfiguration phenomena that involve nanoionic processes [74]. The RS character of the device can be modulated by transport of metal cations to form a nanosized atomic filament across the active insulating material. Similar processes are responsible for atomic scale switching processes [74–76].

3.1. Network dynamics and RS behavior

Emergent dynamics of nanonetworks including collective phenomena arise from local nanoscale effects that regulate the interaction dynamics in between nano-objects and are inherently related to the nanonetwork topology. In this framework, local changes of resistance related to RS effects are responsible for a redistribution of voltages/currents across the network that drives new switching events in different network locations, providing rich spatiotemporal dynamics to these nanoscale systems as discussed in section 4. In this context, different electronic transport mechanisms can regulate the flow of electrons in between two nano-objects: (i) tunneling of electrons in case of nanogaps (ii) ballistic electron transport in case of atomic-sized conductive filament and (iii) Ohmic electronic conduction in case of larger filaments. These electronic conduction mechanisms rely on the interaction between specific nano-objects that can evolve over time. The emergent behavior of the network is related to the dynamic interactions in between nano-objects that give rise to a dynamic reconfiguration of conductive pathways under stimulation. In this context, by analogy with a wide range of complex systems, nanostructured networks can be abstracted as dynamic graphs of interacting nano-objects [44, 77–79], as schematized in figure 2(a). The interactions (links) in between nano-objects (nodes) are regulated by memristive dynamics that rely on RS phenomena at the nanoscale, where the memory state of each memristive interaction depends on the history of applied voltage and current.

Despite several RS mechanisms reported in conventional two terminal memristive devices realized with a top-down approach, RS in nanonetworks can be mainly attributed to the so-called electrochemical metallization memory (ECM) that regulates the interaction in between metallic nano-objects through ion transport at the nanoscale [76, 80, 81], as schematized in figure 2(b). Initially, metallic nano-objects are separated either by an insulating layer or by a nanogap. In case of nanowires, an insulating layer surrounding the metallic core may be formed by a polymeric or an oxide shell layer. Instead, nanogaps are usually present in nanoparticle networks and nanostructured thin films. In both cases, a high resistance in between these nano-objects is expected in the pristine state. When a voltage difference is present in between two adjacent metallic nano-objects, anodic dissolution of metal atoms from the positively charged nanostructure occurs according to the reaction:

$$\mathrm{M} \rightarrow \mathrm{M}^{n+} + n\mathrm{e}^{-}.$$

Consequently, metal ions start to drift across the insulating layer/nanogap towards the nearby nano-object under the action of the applied electric field. When these ions reach the counter nano-object, reduction and deposition of metal ions occur according to the reaction:

$$\mathrm{M}^{n+} + n\mathrm{e}^{-} \rightarrow \mathrm{M}.$$

The deposition of these metal ions results in the formation of a metallic nano-filament bridging the two nano-objects, decreasing the resistance of the interaction. This decrease of the resistance is referred to as a SET event that results in the hysteretic behavior in the I–V plane (cf figure 2(b)). In this framework, the resistance after the SET event is related to the local composition and on the morphology (i.e. size) of the nanofilaments that depends on the applied voltage/current. In addition, kinetics of filament formation and filament morphology is regulated by electrochemical properties of involved

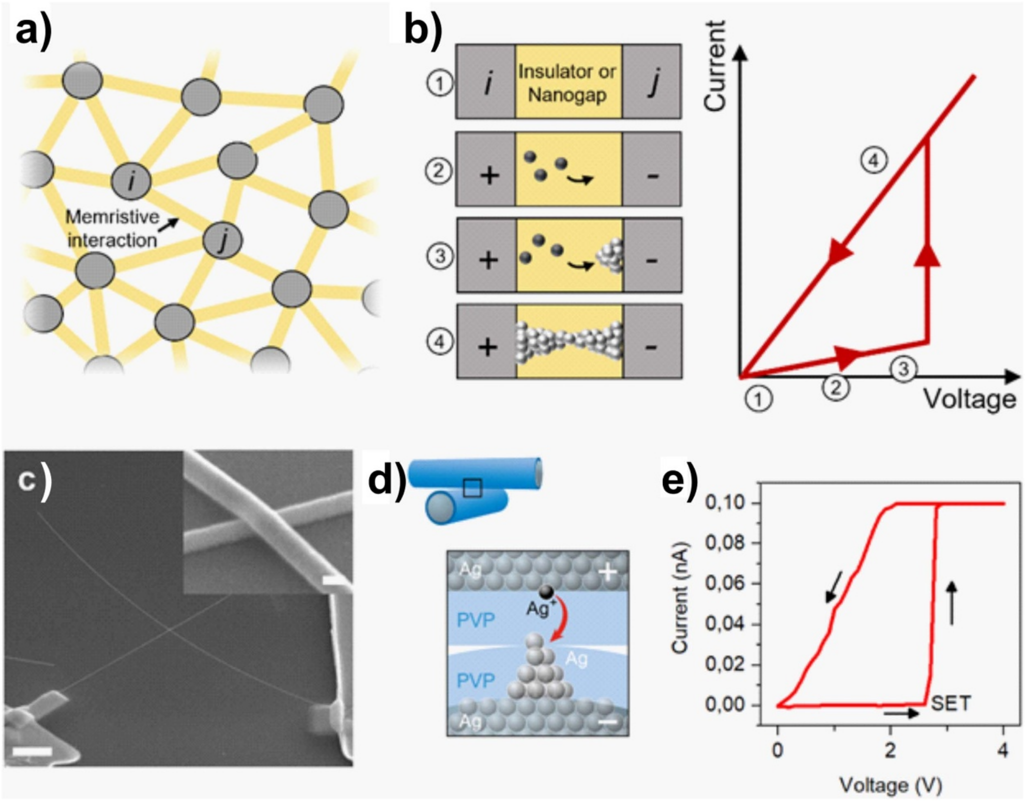

Figure 2. Memristive interactions in between nano-objects. (a) Graph abstract representation of a memristive nanonetwork with memristive interactions in between nano-objects. (b) Schematic representation of the physical mechanism of switching involving the formation of a conductive filament in between two nano-objects under the action of the electric field and corresponding resistive switching characteristic in the *I*–*V* plane. The formation of a conductive filament is responsible for turning the resistance in between the two nano-objects from a high resistance state to a low resistance state. (c) SEM image of a single NW junction fabricated to investigate the memristive interaction in between two nanowires (scale bar, 10 μm). The inset show a detail of the intersection in between NWs where resistive switching occurs. (d) Schematization of the resistive switching mechanism at the NW intersection related to the formation/rupture of an Ag conductive filament across the PVP shell layers connecting the two NW Ag inner cores and (e) experimental resistive switching characteristic of the single NW junction device. Panels (c)–(e) Reproduced from [18]. CC BY 4.0.

materials [82, 83]. This switching mechanism have been reported in a wide range of nanostructures, including single NWs and NW arrays [67, 84–89] (although it is worth noting that physical purely physical electric field induced switching mechanisms are also discussed in the literature—see summary in reference [61]). In this context, nanowire have been reported as suitable model systems for investigating RS mechanisms, including ionic and electronic transport properties, physicochemical phenomena, quantum conductance effects and the role of metal–insulator interfaces, the role of environmental conditions underlying RS and ionic dynamics underlying neuromorphic functionalities of memristive devices [80, 90–99].

The possibility of tuning the filament morphology through the applied electrical stimulation led to an analogue behavior of the interaction, where both formation/rupture of the nanofilament can be viewed as an integration of the applied signals until filament formation/disruption [100]. Taking advantage of these features of the physical mechanism of switching, conventional memristive cells have been largely exploited as artificial synapses and neurons for hardware implementation of brain-inspired computing paradigms [81, 101–103]. Also, it is worth mentioning that the filament formed in between nano-objects can be shrunk down to the atomic scale to form quantum point contacts [61]. Indeed, when the width of these mesoscopic constrictions connecting two electrically conductive regions is comparable to the electronic wavelength, conduction occurs through ballistic electron transport and conductance is quantized in multiples of the fundamental quantum of conductance $G_0 = 2e^2 h^{-1}$. For example, signatures of conductance quantization were reported in percolating nanoparticle films, where experiments and simulations show that the emergent behavior of the nano system arise from the formation of atomic-scale filaments in gaps between particles when the network topology is close to the percolation threshold [61] Similarly, quantum conductance phenomena in between nano-objects were ascribed to be responsible for discrete plateaus of conductance in nanowire networks [23].

Another important aspect is that these conductive filaments connecting nano-objects can break after formation. The filament rupture can be related to (i) a voltage-driven RESET process or to (ii) spontaneous filament dissolution over time, which can be facilitated by local Joule heating. The RESET process can occur when a voltage difference with opposite polarity with respect to the SET process is present, causing the retraction of the previously formed filament. Instead, the driving force of spontaneous dissolution is related to the nanobattery effect that involves the minimization of the interfacial energy through the Gibbs–Thomson effect and electromotive force effects induced by diffusion potential and Nernst potential [80, 81, 104]. Depending on operational conditions during filament formation such as the magnitude of applied voltage and flowing current that regulates the filament morphology, the filament lifetime can range from below the microseconds scale up to months or even years [60, 105].

An example of direct experimental characterization of RS behavior regulating the interaction in between two nano-objects is reported in [18]. Here, the switching behavior regulating the interaction in between two NWs is investigated by fabricating a single NW junction device where two intersecting Ag NWs surrounded by a PVP insulating shell layer have been contacted (figure 2(c)). At the intersection, the physical mechanism of switching is here related to the dissolution of Ag atoms from the NW inner core to form Ag^+ ions that migrate across the PVP shell layers to form an Ag connection in between the two inner cores, as schematized in figure 2(d). Indeed, the single NW junction exhibits memristive behavior characterized by a switch from a high resistance state to a low resistance state under voltage sweep stimulation, as reported in figure 2(e). The switching mechanism was found to be volatile, as testified by the spontaneous relaxation of the NW junction to the ground state after stimulation. Note that similar effects involving the formation and breaking of atomic-scale wires in between nanostructures have been previously reported by Sattar *et al* [61] by experimentally investigating RS in percolating nanoparticle films. Similarly, the formation/rupture of nanoscale filaments in between nano-objects have been suggested to be responsible for the emergent behavior of atomic switch networks [29, 30], nanostructured films [20], nanoparticle networks [20, 28, 106] and nanowire networks [18, 23, 24, 67].

3.2. Nanoparticle systems

In diluted nanoparticle assemblies, RS has been linked to the formation of filaments between individual metal particles, likely resulting from the migration of charge carriers across undoped regions characterized by a moving boundary [21, 28] or attractive van der Waals forces. In many cases the nanoparticles were coated with an organic molecule, oxide or polymer layer, and RS occurred via mechanisms such as redox activity, the formation of a charge-transfer complex, or the creation of donor–acceptor pairs [107]. Self-assembled films of CnS_2-linked Au nanoparticles have electrical properties ranging from insulating to metallic-like depending on the separation of the Au building blocks [108]. In the insulating regime, electric transport is caused by cooperative electron tunneling (co-tunneling) at low temperatures, variable-range hopping at intermediate temperatures, and Arrhenius-type behavior at high temperatures [108]. The influence of each of these mechanisms depends on both the distance between particles and their spatial arrangement [53].

For diluted systems, the percolation theory provides a unified theoretical framework that can be exploited for describing how the structure influence the capability of nanonetworks to transmit information in the form of electrical signals [109].

Percolation on a lattice which contains N sites, in the limit $N \to \infty$, depends on the concentration x of allowed sites. In case of nanonetworks, the concentration x represents the density of nano-objects on the substrate. According to percolation theory, a continuous pathway connecting different areas is present when the concentration exceeds the critical concentration x_c. In case of low concentration ($x \ll x_c$), nano-objects are organized in small and isolated clusters. As x increases, coalescence of particles to form larger groups occurs, until the groups tend to merge when $x \sim x_c$. Consequently, as x approaches x_c, a complete and continuous pathway spanning the system is formed allowing macroscopic flow of information through the system.

From the electrical point of view, three main different topologies can be identified as schematized in figure 3. In case of concentration well below the percolation threshold (figure 3(a-I)), no electrical pathways are expected to connect electrodes contacting the nanonetwork. By increasing the network density, the distance in between neighboring groups of nano-objects is reduced and, even if no continuous pathways are present, electrical conduction in between electrodes can occur through tunneling phenomena that involve transmission across small gaps in incomplete pathways (figure 3(a-II)). This regime, that is not described by classical percolation theory, can be referred as continuum percolation with tunneling since quantum-mechanical tunneling allows electrical transport even before onset of percolation [110]. Instead, higher density networks are characterized by the coexistence of continuous pathways spanning the network and tunneling connections (figure 3(a-III)).

The evolution of the conductivity of cluster-assembled metallic films with thickness can be described by the percolation theory as it has been discussed in the previous section. After the percolation transition, cluster-assembled films are continuous and fully connected (figure 3(a-IV)), however they do not show the electrical behavior typical of continuous metallic films [111]. This is due to inhomogeneity/disorder and the extremely high concentration of defects and grain boundaries slicing the crystal domains that constitute the films [21, 112].

Cluster-assembled metallic films exhibit non-ohmic electrical transport properties with a complex RS behavior [21, 53, 111]. Figure 3(b) reports a schematization of physical mechanisms underlying RS phenomena in nanogranular networks. Depending on the considered material system, a variety of switching mechanisms in nanoparticle networks has been reported. Firstly, in nanogranular network of Ag−, AgAu alloy and Ag/SiO_2 nanoparticles, which are poised at the percolation threshold, the complex RS behavior is traced back to electrochemical metallization mechanism, i.e. reconfigurations of metallic filaments in memristive gaps, which are spread across the network [16, 28, 42]. Secondly, for nanogranular networks from Sn/SnO_x within the regime of continuum percolation with tunneling, atomic migration was found to result in

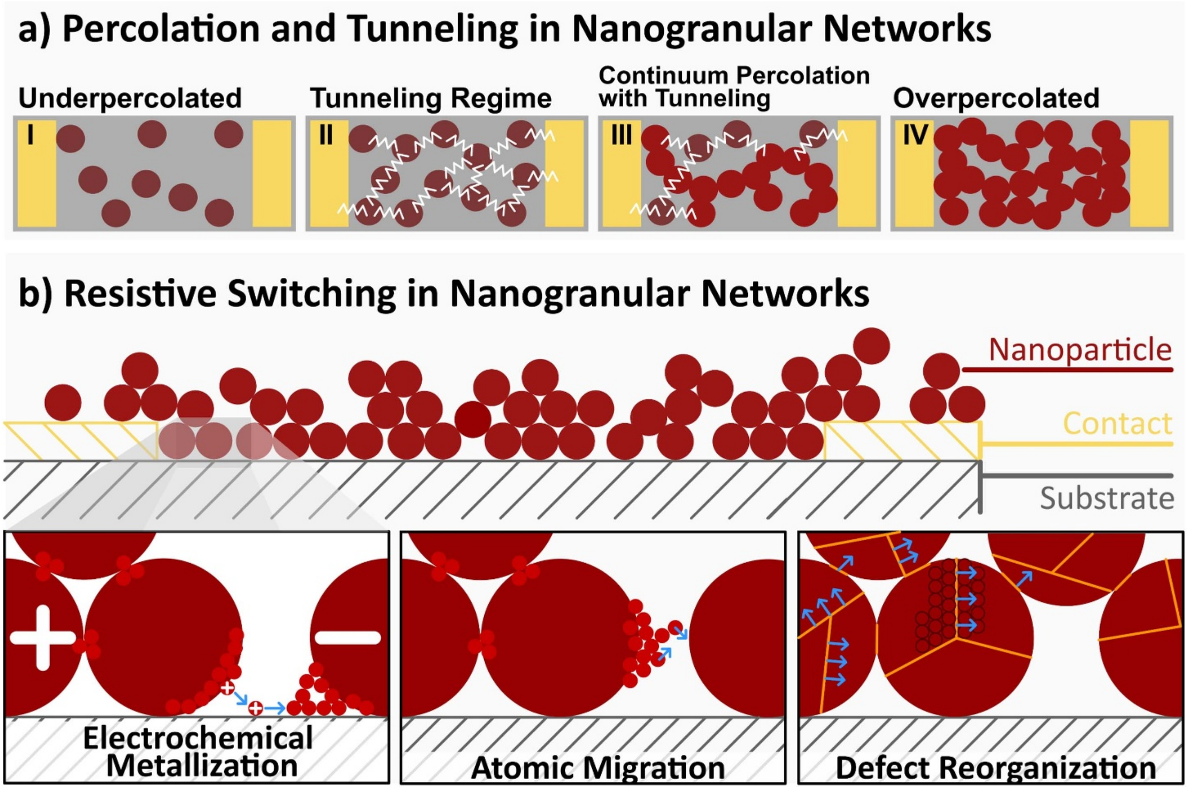

Figure 3. (a) Network topologies and conduction regimes. (I) Low density, nanonetwork of sparsely distributed nanoobjects, where no electrical pathways are present in between electrodes. (II) Tunneling regime observed by approaching the percolation regime, where electrical pathways in between electrodes are provided by transmission across small gaps in non-continuous pathways. (III) Continuum percolation with tunneling observed near the percolation threshold with the coexistence of continuous pathways and tunneling connections. (IV) In highly interconnected network far above the percolation threshold, multiple direct connection pathways between the electrodes are present. Yellow squares represent contact electrodes, white symbols tunneling channels, orange isolated nano-objects while dark red nano-objects forming a continuum pathway; (b) schematic picture of resistive switching processes in nanogranular networks. Depending on the material system there are currently three mechanisms of resistive switching under consideration: (left) electrochemical metallization (i.e. reconfigurable formation of metallic filaments via ionization, transport, and nucleation), (center) atomic migration (i.e. reconfigurable variation of tunnel gap width upon hillock formation) and (right) defect reorganization (i.e. reconfiguration of defect structure involving grain boundaries).

reconfiguration of the tunnel gaps upon hillock formation, Thirdly, the collective reorganization of the defect structure, distributed across the nanogranular network, in particular defects at grain boundaries, has been reported and systematically characterized in the case of cluster-assembled Au films [53, 113].

The non-linear electric behavior and, in particular, the non-local effects in continuous cluster-assembled metallic films are related to nanoscale structural change of the network characterized by the presence of an extremely high density of defects, dislocation, and grain boundaries typical of cluster-assembled films [21, 53, 112, 114]. Cluster-assembled films are characterized by a grain distribution substantially similar to that of the sub-monolayer regime [115].

Electronic carrier conduction in these systems can be considered to be based on space charge limited conduction mechanisms and coulomb blockade [112]. The effect of Coulomb blockade becomes particularly prominent at temperatures far below room temperature. The presence of an extremely high density of grain boundaries and crystalline orientation mismatch deeply affect the electrical conduction [116] representing a barrier for the electric charge flow determining and resulting in a distribution of different 'resistances' over the cluster-assembled film.

Structural inhomogeneities correspond in variation of the local resistance at the nanoscale: numerical simulations [117] suggest that scattering phenomena through grain boundaries under a flowing electron current can cause the formation of 'hot' spots with a high local temperature compared to regions at low resistance where the temperature is lower. This causes defect migration, grain boundaries modification and annealing, nanoparticle internal reorganization that take place at different temperatures due to the different nanoparticle dimensions and structure [53, 118–121] (figure 3(b)).

4. Emergent neuromorphic functionalities

A characteristic feature of the brain's neuronal circuitry is its ability to adapt to continuously changing signals, which has been attributed to collective nonlinear dynamics [122]. Dynamical phase transitions, for example, are considered to confer a functional advantage to complex systems with neural-like adaptive dynamics [123–125]. This section highlights some of the emergent brain-like properties that have been identified in self-organized networks of memristive nano-elements and their implications for information processing.

4.1. Nanoparticle networks

Nanoparticle networks provide a system for neuromorphic computing in which the properties of networks are exploited, rather than those of the particles themselves. These networks can broadly be categorized according to whether the particles are embedded in a matrix or are randomly deposited on a flat surface (with no matrix). In the former case the result is a nanocomposite [126] and in the latter case the result is a percolating network.

In the context of neuromorphic computing, the fabrication of networks of nanoparticles usually relies on the deposition of pre-formed particles (often called 'clusters'), from a beam [46, 127, 128]. In the cases of interest here the particles are randomly deposited in a 2D plane (experimentally, this is usually between electrodes on a silicon substrate) and it is immediately clear that concepts from percolation theory apply. It was shown very early that atomic deposition and nanoparticles deposition lead to very different kinds of percolation behavior [46]. (We note in passing that that atomic deposition can be used to produce other devices which are also composed of nanoparticles, such as quenched-condensed or discontinuous films, but these are much less well-investigated for neuromorphic applications (see [129] and references therein).

Initial experimental studies of percolating nanoparticle networks were focused on demonstrating that the power–law dependences of key quantities expected from theory [130] could in fact be observed. Schmelzer *et al* [128] were able to directly observe the percolation threshold (as a sharp change in conductance, when the nanoparticle network spanned the space between the electrodes) using carefully designed devices comprising two pairs of interdigitated electrodes, with different spacings. The percolation threshold was shown to exhibit the expected shift with system size and it was also shown that the critical exponent for the correlation length was consistent with predictions [128]. Subsequent work [131] showed that, in the regime $p > p_c$, the critical exponent for the conductivity was consistent with theoretical predictions from percolation theory for devices formed from Ag and Bi nanoparticles, but that devices formed from Sb particles exhibited different power–law exponents because in certain regimes the particles bounce of the substrate. These bouncing effects [132–134] were later used as the basis for several methods of forming nanowire [135–137].

An important aspect of the work mentioned so far in this section is that it established that the properties of nanoparticle devices could be understood in terms of continuum percolation i.e. that they were entirely equivalent to those of randomly deposited disks in two dimensions [128, 131]. The device properties were not significantly affected by coalescence or diffusion effects [138], or by stacking of nanoparticles on top of each other during deposition. In this regard it is worth emphasizing that for 2D continuum percolation, the percolation threshold at $p_c \sim 0.68$ (i.e. projected surface coverage in the 2D plane) corresponds to a total coverage $p_{tot} \sim 1.1$ (i.e. total including the overlap of disks/particles deposited on top of others). Since p_{tot} is only ~35% greater than p_c, stacking effects are unimportant near the percolation threshold and only really become significant for $p \gg p_c$ [131]. The overlap between deposited disks/particles does however lead to the formation of groups of particles separated by tunneling gaps, as shown in figures 4(a)–(d).

4.1.1. Neuromorphic behavior at the percolation threshold. The first evidence for memristive switching behavior in percolating Bi nanoparticle films was observed in very early experiments [139], however the significance of these effects was not appreciated at the time—they were reported more than 5 years before the 'discovery' of the memristor [140]. It was another decade before it was possible to observe this switching behavior reproducibly in large numbers of devices [61]. It was realized that it was necessary to focus on films of nanoparticles that were close to the percolation threshold, when tunnel gaps are present in the film. Using complementary simulations, the observations of switching and of quantized conductance at room temperature were explained as the result of the formation of atomic-scale wires in the gaps between particles (quantized conduction requires that a conducting channel has dimensions of the Fermi wavelength, which for metals is atomic scale) [61]. This work therefore led to a new focus on percolating-tunneling systems i.e. on 2D continuum percolation near to p_c, where the influence of tunneling through the gaps between particles was considered in addition to the usual conducting pathways (formed from connected nanoparticles).

Perhaps surprisingly, percolating systems with tunneling were relatively unexplored at that point, and basic questions, such as whether a sharp conduction threshold (second percolation threshold) should be observed in systems where tunneling was allowed, were unresolved [141]. These questions were definitively addressed by simulations [110, 142], which showed that tunneling leads to an approximately exponentially decaying current at low surface coverages, and that the jump to metallic conduction at p_c is superposed on this tunneling current. Subsequent simulations [143] showed that an applied voltage can cause the formation of a continuous conducting pathway due to the formation of atomic scale filaments in multiple gaps across the film, a result that was later mirrored experimentally by the demonstration of winner-takes-all (WTA) pathways in nanowire networks [23].

The discovery of the memristor [140], and subsequent demonstration of neuron-like and synapse-like behavior in various memristive (and other) devices [144] motivated further investigation of percolating-tunneling devices. Early devices, built using tin nanoparticles, were fragile and it was difficult to achieve reproducible behavior [61]. These problems were solved by the discovery that exposure of the Sn particles to small amounts of air and moisture during deposition led to control of oxidation and coalescence processes, and hence to devices that were stable for many months [60, 145]. This

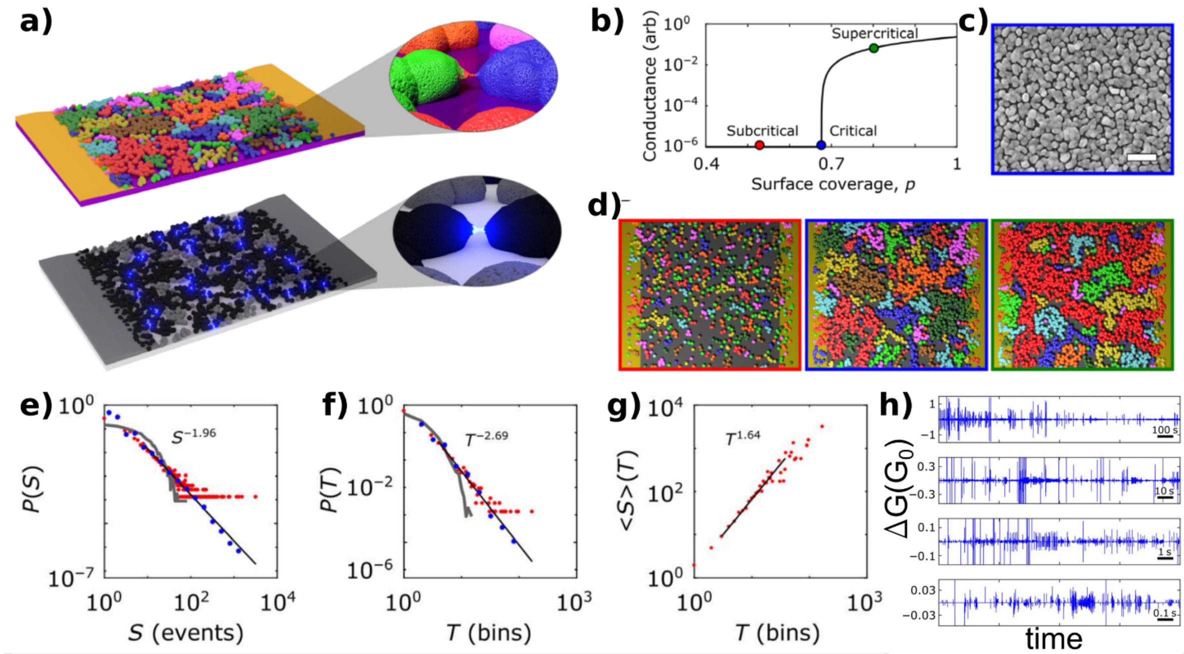

Figure 4. (a) Top: schematic diagram illustrating our simple two-terminal contact geometry and a percolating network of nanoparticles. The different colors represent groups of particles that are in contact with one another. The zoomed region shows a schematic of the growth of an atomic filament within a tunnel gap (switching event) when a voltage is applied. Bottom: the same network schematic presented so as to show the conducting pathways (black) that result from atomic filament formation within the gaps between groups. (b) Schematic showing the conductance of a device during deposition of conducting nanoparticles follows a power law $\sim(p - p_c)^{1.3}$ (the critical surface coverage is $p_c \sim 68\%$). arb, arbitrary units. (c) A scanning electron microscope image of a percolating nanoparticle network. Scale bar, 200 nm. (d) Schematic diagrams showing the following: left—in the subcritical, insulating phase at low coverage, groups of particles are small and well separated, so that if an atomic switch connects two groups, then there are few possibilities that this will trigger another switching event; right—in the supercritical, conducting phase at higher coverages, highly connected pathways across the network mean that when an atomic filament bridges a tunnel gap, an avalanche can propagate only to a few nearby tunnel gaps; center—in the critical phase, avalanches propagate on multiple length and time scales. (e)–(g) Avalanche criticality in nanoparticle networks. (e) Probability distribution of avalanche size S. (f) Probability distribution of avalanche duration T. (g) Average size as a function of duration. Red and blue data points represent linear and logarithmic bin sizes, respectively. Maximum likelihood power–law fits are shown in each case. (h) Self-similar conductance changes on various time scales indicate scale-invariance. From [20]. Reprinted with permission from AAAS.

allowed long term measurements of the devices and hence to the possibility that comparisons could be made with data obtained from biological systems. Further improvements to the stability of nanoparticle networks were observed in systems based on Ag nanoparticles and, in particular, AgAu alloy nanoparticles, which enabled operation at room temperature and in ambient air for multiple months [16, 28].

Detailed investigations revealed that, near the percolation threshold, networks of tin nanoparticles exhibited correlated avalanches of signals [20], similar to those observed from the network of neurons in the cortex [146]. The avalanches of signals were shown to exhibit scale-free dynamics over many orders of magnitude (see figure 4(h)), and detailed analysis showed that the sizes and durations of the avalanches are power–law distributed (see figures 4(e) and (f)). Moreover, this analysis showed that the avalanches exhibited classic signatures of criticality (see figure 4(g)) [147] i.e. that the measured power–law exponents satisfied the crackling relationship, and that the dependence of the mean size of the avalanches on duration and shape collapse yielded consistent estimates of the critical exponent $1/\sigma\nu z$, as required for criticality [20]. These results are significant as criticality has been extensively studied in neuroscience to test the hypothesis that the brain achieves optimal computational performance when in or near a critical state [148–150]. In that context, avalanche criticality refers to the statistical properties of action potential (voltage spike) events typically measured in cortical neurons [151–153]. In percolating-tunneling Sn nanoparticle networks, avalanches are measured as spike-like conductance switching events [20, 78].

Since critical systems are suggested to provide opportunities for optimal information processing capabilities [154, 155], percolating networks of nanoparticles are promising systems for brain-like computing. Importantly, similar demonstrations of criticality have been achieved for Ag nanoparticles, even when embedded in an oxide matrix [28], suggesting that criticality is a general property of networks of nanoparticles at the percolation threshold, and providing a pathway toward real-world devices. In that regard it is worth mentioning that one of the attractions of these self-assembled devices is that the processes used are entirely CMOS compatible, and are therefore amenable to integration in larger scale systems, such as those intended for, for example, edge computing.

Further investigations of percolating networks of tin nanoparticles have included detailed analysis of long-range temporal correlations within the networks, and comparison with equivalent data from biological systems [78]. It was shown that the long-range correlations derived from a scale-free network architecture [78], in combination with neuron-like atomic-scale integration and fire processes within the tunnel gaps in the percolating network [106]. Simulations are invaluable in demonstrating the mechanism for the observed correlated avalanches: as in the biological brain [156], where when one neuron fires it triggers (on average) one other neuron, in the percolating networks one switching event triggers another. It is the formation (or breaking) of an atomic scale filament in one tunnel gap that triggers another filament to be formed (or broken) in another. Interestingly, a dynamical balance (a possible self-organized critical state) is achieved since if, due to random fluctuations, the number of connections in the network becomes too few (or too many) the system tends to drive the formation of more (or fewer) filaments and drives the conductance of the network as a whole towards a stable value [106].

More recent work on percolating networks of nanoparticles has focused on multi-contact devices, which are designed to allow multiple input and output signals to be provided to (read from) the networks [27]. Such devices are obviously required in order to implement computational schemes such as reservoir computing (RC) (section 5.1) but alternative schemes are important and steps towards exploitation of spiking activity for computation have already been made [157]. Experiments have initially focused on demonstration of the basic properties of the multi-contact devices, and in particular on showing that criticality is maintained. This work addressed concerns that different contact configurations might bias the network in such a way as to destroy correlations. (Further simulations, of nanowire networks [19, 158], have addressed other practical questions about the optimal choices of parameters such as the number of electrodes and size of the system.) Recent simulations [159] have shown that in fact criticality is affected only in relatively small devices for a relatively small number of pathological contact configurations. This work also showed that repeated switching in the same gap can be expected when the current paths in the nanoparticle network are focused through a small number of tunnel gaps that connect nearby electrodes. Interestingly, exactly this behavior is observed experimentally [27]: in multi-contact devices the current measured at individual electrodes can exhibit long sequences of identical spikes, from a single 'neuron'. The times between spikes are found to be stochastic (as in the biological brain), and this stochasticity has been exploited for high quality true random number generation [27]. Hence percolating networks of nanoparticles may have unexpected applications in stochastic computing and secure information processing [160], in addition to those in neuromorphic computing.

4.1.2. Neuromorphic behavior beyond the percolation threshold. The behavior of continuous metallic cluster-assembled films beyond the percolation threshold has been extensively investigated in the case of nanostructured Au films [21, 111, 113]. Continuous Au cluster-assembled films are non ohmic with a discrete variation of the resistance (figure 5) and characterized by the presence of a switching activity with a series of discrete and reversible resistance variations; the *I*–*V* curve shows a non-linear behavior and the presence of hysteresis [21, 111, 113].

The films can change reversibly and reproducibly their resistance from different high to lower levels depending on the applied voltage (figures 5(a)–(c)); reversible switching behavior can be controlled tuning the pulse width and the height. In figures 5(e)–(g) consecutive and reversible switch between higher and lower resistance state are shown with the applied pulses.

Inter-switch-interval (ISI) distribution analysis as in the case of neuronal networks have been used to verify the existence of a degree of correlation among the electrical spikes observed in the cluster-assembled films [20, 161]: typical ISI distribution is shown in figure 5(h).

RS events in nanostructured metallic films are observed also at cryogenic temperatures [112]: this could be related to the structure of cluster-assembled films characterized by a landscape crowded of defects and interconnects between grains resulting in an assembly of interacting nanojunctions [53]. Multiple conductance states are observed in single metallic nanojunctions at cryogenic temperatures with electrical conductions characterized by discrete steps of conductance involving Coulomb blockade phenomena both in increasing and decreasing resistance [162].

4.2. Nanowire networks

Similar to the case of nanoparticles, also in case of NWs the interest in the field of neuromorphic computing is mainly related to the exploitation of the emergent properties of networks of NWs rather than those of the NW itself. In this framework, pioneering works showed that randomly interconnected networks of Ag_2S nanowires act as self-assembled atomic switch networks able to emulate neuromorphic functionalities [29, 30]. In this context, it was proposed that these networks can be similar in structure to Turing's 'B-Type unorganized machine' as randomly connected networks of logic gates [36]. The aim of this seminal work was mainly to emulate the structure and activity of the biological brain including spatially distributed memory, recurrent dynamics, and scale-free fluctuations, rather than on the implementation of computing paradigms. Subsequent studies of these NW networks also revealed higher harmonic generation under an AC bias [69], which led to the demonstration of waveform regression tasks using RC (see section 5.1) [163]. Similar collective behaviors have since been observed in single-walled CNTs [164]. Inspired by neuroscience and motivated by unveiling the interplay in between structure and function of these self-assembled systems, growing interest was then devoted in understanding the interplay in between the NW network topology and emergent memristive functionalities [44, 77, 158], together with emulation of synaptic functions and physical implementation of unconventional computing paradigms such as RC (see section 5) [15, 19, 26, 165, 166]. Beyond RC, it was also demonstrated that NW networks can emulate higher-order cognitive functions such as working memory [167].

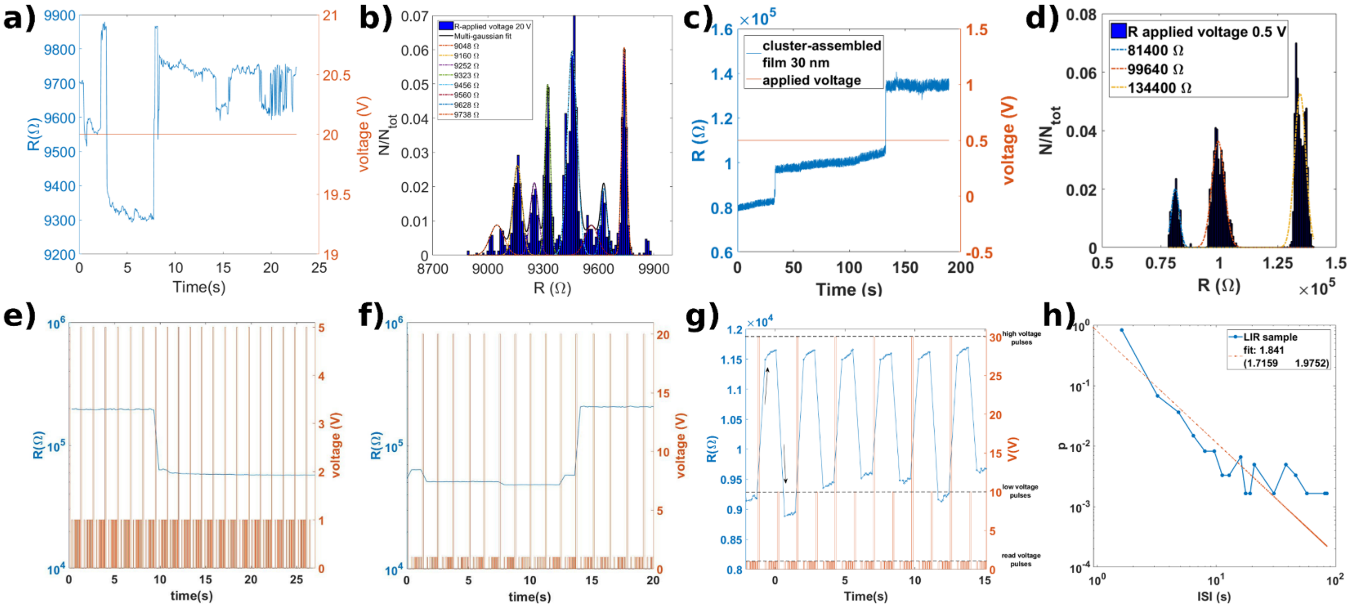

Figure 5. Example of resistive switching behavior in cluster-assembled gold films. (a) Electrical resistance of a film with thickness of 30 nm under a bias of 20 V; (b) histogram of the resistance values under the application of 20 V in a time window of 200 s. (c) Electrical resistance of the same sample under a bias of 0.5 V. (d) Histogram of the resistance values of the sample under the application of 0.5 V in a time window of 200 s; (e) transition to a low resistance level under the application of low voltage pulses (5 V); (f) transition to a higher resistance level under the application of high pulses (20 V). Y axis in log-scale for both graphs; (g) an example of consecutive transition from the higher resistance level to the lower one and vice-versa observed under the application of consecutive low (10 V) and high (30 V) voltage pulses; (h) ISI distribution: the power law obtained by the maximum likelihood method is shown in the log–log scale graph (the estimated parameter with the confidence bounds at 95% certainty level is shown in the legend). Panels (a)–(d) Reproduced from [111] with permission from the Royal Society of Chemistry. Panels (e)–(h) Reproduced from [21].

4.2.1. Nanowire network topology. From social networks to electrical power grids and biological systems, the network topology is intimately related to functionalities [168]. In the framework of network science, NW networks can be represented as mathematical objects on the basis of graph theory [44, 77, 79, 158]. The NW network, modeled as a network of 1D sticks randomly dispersed on a 2D plane can be abstracted as a graph where nodes and edges represent NWs and NW interactions, respectively. In the work by Loeffler *et al* [77], network cartographic approaches borrowed from neuroscience were exploited to compare neuromorphic nanowire networks with random networks, grid-like networks, and the structural network of the *Caenorhabditis elegans* biological system. Results showed the NW networks exhibit small-world architecture that is similar to the biological system of *C. elegans*, while significantly differing from random grid-like networks as well as from the architecture of untrained ANNs. In addition, it was shown through simulations that stacking of the NWs strongly influences the network topology [158]. The stacking effect in real-world NW networks leads to the formation of quasi-3D network as a consequence of the deposition process, with a much weaker 'small world character' in real-world quasi-3D networks than in perfectly 2D networks. In other work [44] it was shown that graph metrics are linked to purely geometrical considerations and that results from graph theory agree with percolation theory. By considering NW networks as memristive graphs and by analyzing the interplay in between the network structure and its capacity to transmit information, the concept of memristive distance was introduced to describe the dynamic evolution of the effective resistance in between two graph nodes. In agreement with experimental results, modeling showed the emergence of self-selected pathways that connect the stimulating areas, regulating the trafficking of the information flow across the network.

4.2.2. Emergent memristive behavior of nanowire networks. The emergent memristive behavior of NW networks arises from RS events occurring between NW network elements, where changes in the conductance across NW–NW junctions result in a redistribution of current/voltage across the whole network causing collective phenomena [24, 169]. In particular, memristive behavior in NW networks have been reported to be related to 'reweighting' and 'rewiring' effects that can occur in NW junctions and single NWs, respectively, as experimentally investigated by Milano *et al* [18] in devices based on single NW junctions and single NWs.

The 'reweighting' effect refers to RS phenomena at NW junctions in between intersecting core–shell NWs, where the formation/rupture of a metallic filament connecting the two metallic cores occur under the action of an electric field according to the ECM mechanism detailed in section 3. In this context, it is worth noticing that experimental results obtained in single NW junction devices evidenced that the pristine state of NW junctions can span over several orders of magnitude of resistance because of the mechanical stochasticity of the contact in between intersecting NWs [18]. In addition, it was shown in a previous work that [23] the internal state of NW junctions can be programmed to different resistance states in an analogue fashion by adjusting the imposed compliance current. Moreover, it was shown that the symmetric structure of NW junctions allows the filament to grow or decay by applying both voltage polarities to inner cores of intersecting NWs [18].

The 'rewiring' effect refers to the rupture of NWs that can occur in single NWs under electrical stimulation [18]. In this case, electrical stimulation can lead to the rupture of single NWs to form a needle-like nanogap due to Joule heating and electromigration-driven electrical breakdown. The electrical connection in between the two disconnected parts of the NW can be then restored thanks to electromigration phenomena involving the formation of a conductive filament in the previously formed nanogap under the action of an applied electric field. Thus, the rupture/rewiring of the nanogap can be responsible for RS in single NWs.

Reweighting and rewiring effects in memristive nano components thus contribute to an emergent memristive behavior of the NW network at the macroscale. When an electrical stimulation is applied in between any two areas of the network, current flows across connected NWs in accordance with Kirchhoff's laws and is regulated by the conductance state of each memristive element of the network. Changes in the conductance of a memristive element causes the redistribution of current and voltages across the entire network, causing other changes in the conductance state of connected memristive elements through a cascade effect. Under AC stimulation, this causes the emergent memristive behavior of the NW network characterized by the typical hysteretic loop in *I–V* curves, as shown in figure 6(a)) in case of Ag NW networks [18]. Under multiple AC cycles, the response is consistent with attractor dynamics [123, 170], which has been identified as central to the brain's computational abilities [171]. Under DC stimulation, cascading switching activity, tempered by stochastic fluctuations that rupture conductive nano-filaments, was found to exhibit avalanche criticality. This was shown in both Ag-PVP [126] and Ag_2Se NW networks [170] using different devices operating in a two-terminal configuration: a double-electrode device and a multi-electrode array (using a single source-drain pair), respectively. The critical exponents measured from the avalanche statistics differ for the two different NW systems and also differ from those measured for Sn NP networks, which may indicate different universality classes or departure from a single critical point. These findings open up new opportunities for testing the criticality—computation hypothesis in physical abiotic substrates, which may in turn reveal new insights into the role of criticality in the brain [172, 173].

The emergent memristive behavior of NW networks is related to the emergence of spatially correlated network areas with enhanced conductivity under stimulation, with the emergence of conductive pathways connecting stimulating electrodes. Manning *et al* reported a direct investigation of conductive pathways formed in Ag NW networks under electrical stimulation by means of passive voltage contrast SEM imaging as reported in figure 6(b) [23]. By using this technique NWs that belong to the conductive pathway created through electrical stimulation that connect stimulating electrodes appear to be darker while disconnected (or less-connected) NWs appear to be brighter [23] (A similar demonstration of pathway formation in NP networks was reported earlier [143]). By showing the dependence of the conductive pathway morphology on the applied compliance current, this work experimentally proved that the morphology of the conductive pathway can be regulated by tuning the electrical stimulation. In this work, it was proposed that a 'winner-takes-all' (WTA) conduction regime can occur in NW networks, where the WTA path can exhibit stable conductance plateaus and represent the lowest possible energy connectivity pathway in the network. In a later work, Li *et al* [174] reported on the direct visualization of conductive pathway in Ag NWs decorated with TiO_2 nanoparticles through lock-in thermography. Here, it was shown that for sufficiently high voltage/current, an enhanced IR radiation related to Joule heating effects is emitted locally in correspondence of the conductive pathway formed across the NW network. Also, it was shown that the NW network conductivity can be mapped through Electrical Resistance Tomography that allows to reconstruct the conductivity map of the network through boundary electrical measurements [175–177]. This technique experimentally allowed to observe the evolution of the connectivity map under electrical stimulations, allowing to map spatiotemporal changes of the conductivity in nanonetworks under external stimulation. It is worth mentioning that, before these works, it was already reported the possibility of locally manipulating the connectivity of NW networks by c-AFM. Indeed, Nirmalraj *et al* demonstrated that a metal coated AFM tip can be exploited to locally activate network areas by applying a voltage stimulation, demonstrating that networks realized with both PVP-coated Ag NWs and surface-oxide-passivated Ni NWs can be programmed to create materials with control of local connectivity at the nanoscale [68].

Under proper operational conditions, it was demonstrated that conductive pathways formed across NW networks can be volatile [15, 18, 24]. This behavior is related to the spontaneous dissolution of conductive filaments in memristive elements composing the networks (details in section 3), with consequent dissolution of the conductive pathway spanning the network after the end of stimulation. In this case, the NW network endows short-term memory and the effective resistance in between stimulating areas tends to restore the pristine resistance state over time. An example of short-term memory of an Ag NW network stimulated in two-terminal configuration with a voltage pulse is reported in figure 6(c). While the effective conductance progressively increases due to the formation of a conductive pathway during voltage pulse stimulation (potentiation), relaxation of the effective conductance towards the ground state can be observed after the end of stimulation due to short-term memory effects (spontaneous relaxation). It is worth noticing that spatio-temporal dynamics based on short-term memory effects in NW networks are crucial for the emulation of synaptic functionalities, for information

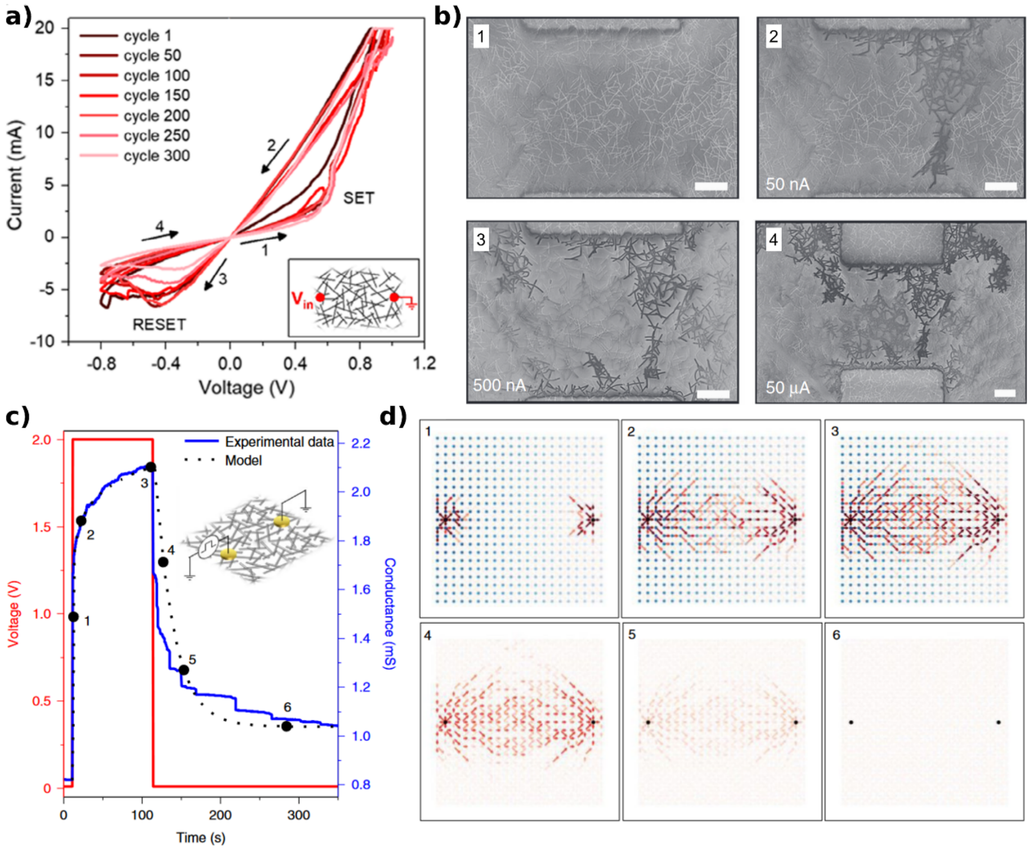

Figure 6. Emergent memristive behavior of NW networks. (a) Resistive switching behavior of a NW network measured in two-terminal configuration, as schematized in the inset, showing the typical hysteretic loop of a memristive device. Reproduced from [18]. CC BY 4.0. (b) Direct investigation of conductive pathways formed in Ag NW networks under electrical stimulation by means of passive voltage contrast SEM imaging. Images were acquired on the same network stimulated with I–V sweeps by imposing different limiting current compliances in between the two metal contacts (top-left panel shows an unperturbed network). Scale bars correspond to 2 μm. Reproduced from [23]. CC BY 4.0. (c) Experimental and simulated potentiation during voltage pulse stimulation and following spontaneous relaxation of the effective conductance of an Ag NW network measured in two-terminal configuration and (d) corresponding evolution of the conductivity map obtained through grid-graph modeling. Panel (c), (d) Reproduced from [15] with permission from Springer Nature.

processing and for the implementation of computing paradigms such as RC (refer to section 5.1). Under longer DC stimulation and persistent volatility, NW networks have demonstrated fault tolerance, with an ability to maintain functional integrity and resilience against localized damage caused by continual reweighting and rewiring [24]. This resilience is attributed to the remaining parts of the network compensating for the part that has been functionally disrupted, as inferred from observations of a rapid recovery in network conductance following a sudden drop.

To better understand how the internal dynamics of NW networks relate to their emergent memristive properties, modeling and simulation studies have provided valuable insight. A grid-graph model where the memristive behavior is decoupled from the particular and detailed behavior of each network element has been proposed [15, 178]. This model approximates a high-density NW network as a 2D continuous medium that is then described as a regular grid-graph with memristive edges, where the dynamics of each memristive edge are regulated by an analytical potentiation-depression rate balance equation that takes into account short-term memory effects [179]. Besides allowing direct interpolation of experimental results, this model allows visualization of the spatio-temporal evolution of the conductive pathway when electrically stimulated in specific spatial locations as reported in figure 6(d). The potentiation-depression rate balance model for the memristive edges was subsequently shown to be compatible with a theoretical mean-field approximation for random networks [180], which was further validated against experimental measurements [181]. An alternate model, developed for Ag-PVP memristive NW networks, instead solves Kirchhoff's laws for arbitrary network connectivity structures using the adjacency matrix and graph Laplacian [123, 182]. This approach enables simulation of dynamic networks with a broader range of densities, from the low-density percolation limit (sparse networks) to high-density random networks. In this case, edges are modeled as voltage threshold-driven bipolar ECM memristors, with conductance switching triggered by tunneling. Simulation studies using this model have revealed how synchronization of memristive switching events forms the initial WTA conduction path under a DC bias [123], which is similar in nature to transient synchrony in the brain [31]. It was also shown that the WTA path is concomitant with a discontinuous transition in conductivity, as also found in other modeling studies [183].

Overall, the dynamical phase transitions, attractor dynamics and synchronization associated with the emergent memristive properties of NW networks resonate with Hopfield's [184] proposition that new computational capabilities can spontaneously emerge from the collective dynamics of large numbers of relatively simple processing elements, as discussed in the following section.

5. Nanogranular networks for computing

There are many possible approaches to exploitation of the properties of nanogranular networks in emerging computation scenarios, including spiking computation for Boolean logic and image classification [157]. In this review, we focus on nanogranular networks as physical reservoirs for RC (cf section 5.1) and receptrons as reconfigurable Boolean function classification devices (cf section 5.2).

5.1. Physical RC

RC represents a computational framework derived from recurrent neural network (RNN) models such as echo state networks [185] and liquid state machines [186] where computation is divided in two sections: the 'reservoir' and the 'readout' [187, 188]. The 'reservoir' projects temporal input signals into a new feature space that represents a nonlinear transformation of the input, while learning is performed in the 'readout' layer that analyzes the reservoir state and generate the output of the system. As conceptually schematized in figure 7(a), the reservoir maps a time-dependent input $u(t)$ into a feature space that is represented by the internal state of the reservoir $x(t)$ that is then analyzed by the readout, where readout weights are trained by comparing the output $\hat{y}(t)$ with the desired output $y_{\mathrm{d}}(t)$. Since only the weights of the readout need to be trained no training is required for the reservoir, this computational framework substantially reduces the computational cost of learning and is highly versatile.

Since the basic concept of RC is to exploit intrinsic dynamics of the reservoir by outsourcing learning, reservoirs can be directly realized by exploiting the dynamics of physical systems instead of using simulated dynamics of an algorithmic RNN. The computational framework where the reservoir is realized by exploiting intrinsic dynamics of physical systems and computation is performed 'in materia' [15] this approach is referred as physical RC [187, 188]. This emerging research field involves not only the machine learning and artificial intelligence community but also the field of physics, dynamical systems, material science, biology, and neuroscience. With the aim of exploring the computational power of physical systems, physical RC has been implemented by exploiting mechanical, photonic, spintronic, and electronic systems [187, 188]. By exploiting internal ionic dynamics of memristive cells where the internal state of resistance depends on the history of applied voltage and current, physical implementation of RC have been demonstrated also in arrays of memristive devices realized with a top-down approach [189, 190].

In the present context, self-assembled networks of interacting nanoobjects have been demonstrated as suitable platforms for the implementation of RC by emphasizing the network architecture as a whole, exploiting the emergent dynamics of the system without fine tuning of its elements. While pioneering works explored the implementation of RC using CNTs [191, 192] and self-assembled atomic switch networks [60], this approach was then adopted in a wide range of self-assembled systems including NW networks [15, 26, 165, 193–195], NP networks [196–198], molecular networks and organic electrochemical networks [199, 200]. In all these cases, the reservoir state is represented by the collective state of network elements.

In the case of NW networks, Sillin *et al* [26] demonstrated the realization of a kernel for RC based on an atomic switch network of intersecting NWs, where the dynamics can be regulated by controlling the network connectivity density. Milano *et al* [15] demonstrated experimentally that the emergent behavior of NW networks endows nonlinear dynamics and fading memory properties, key prerequisites for exploiting these systems as physical reservoirs. Simulations by Zhu *et al* [182] demonstrated enhanced information processing (quantified by task performance and information theoretic measures) when memristive NW networks were prepared in a state near the dynamical phase transition in conductivity. A learn-to-learn strategy has also demonstrated how RC may be optimized using these networks [201]. In a converse approach using simulated networks of nanoscale spintronic oscillators, Feketa *et al* found that an evolutionary search driven solely by task performance led the network toward a critical state [202]. In this context, NW networks have been reported for solving a wide range of computing tasks including waveform generation [26, 30], pattern recognition [15], time series prediction [15] and speech recognition [166, 194]. Similarly, waveform generation through physical RC was demonstrated in NP networks [188] and time series prediction and classification were achieved firstly in simulations [196] and then in experiments which also extended the approach to speech recognition tasks [198].

RC at the edge-of-chaos, a state between ordered and chaotic dynamical regimes, has also been investigated using NW networks [123, 203, 204]. The edge-of-chaos does not necessarily coincide with criticality and in the case of NW networks, the two dynamical regimes are distinct: while avalanche criticality (activity propagation) is triggered by sustained fluctuations under a DC bias, the order-chaos transition is instead reached under strong AC driving. In a simulation study, Hochstetter *et al* [123] demonstrated that a NW network in an edge-of-chaos state (with maximum Lyapunov exponent $\lambda \approx 0$) performed better than when in an ordered ($\lambda < 0$) or chaotic ($\lambda > 0$) state, but only as task complexity increased (see figure 7(b)). This result is similar to a study of a spiking RNN, which found that only complex tasks benefit from criticality [205]. Interestingly, that study used leaky integrate-and-fire point neurons, whereas Hochstetter *et al* used a conductance-based model that effectively replaces the

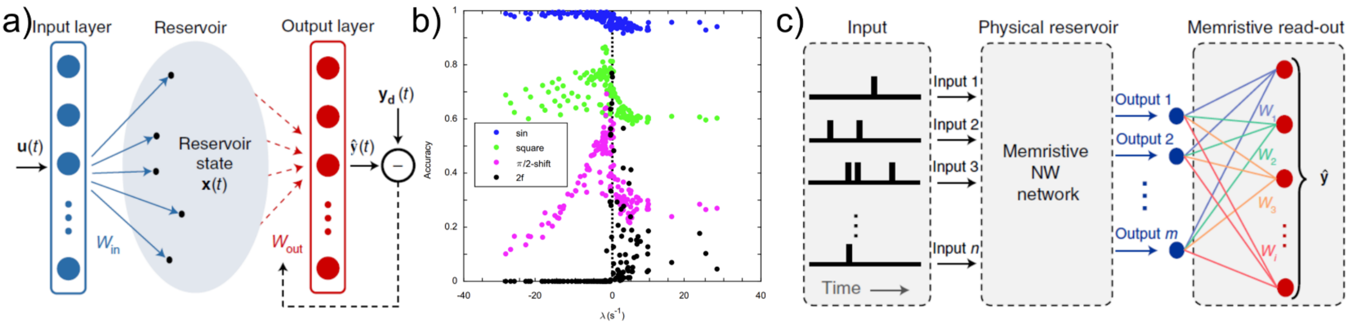

Figure 7. (a) Schematic representation of the RC paradigm where the reservoir maps the input $u(t)$ in the reservoir state $x(t)$ through input weights W_{in}, while output weights W_{out} are trained by comparing the output $\hat{y}(t)$ with the desired output $y_{\text{d}}(t)$. Reproduced from [15] with permission from Springer Nature. (b) Edge-of-chaos learning in nanowire networks. Simulated waveform regression task accuracy as a function of maximum Lyapunov exponent λ for transformation of an input triangular wave into target waves with Fourier components of varying complexity. Vertical dotted line indicates $\lambda = 0$. Reproduced from [123]. CC BY 4.0. (c) Schematic conceptualization of the fully memristive implementation of reservoir computing where a physical reservoir based on a self-organizing memristive NW network is coupled with a memristive readout composed of ReRAM devices realized with a top-down approach. Reproduced from [15] with permission from Springer Nature.

leaky capacitor with a voltage threshold-driven memristor, where leakage is due to tunneling. Performance enhancement at the edge-of-chaos was also reported using an ion-gating reservoir [75]. These studies, together with those mentioned above, indicate that for brain-inspired computing, the collective dynamics are at least similarly important as the specific details of the neuron-like dynamics of individual nanoscale elements [170].

The computing capabilities of these self-assembled networks are also intrinsically related to the network topologies. By analyzing the performances of NW networks on two benchmark computing tasks, memory capacity and nonlinear transformation, Loeffler *et al* [206] showed through simulations that NW networks with a highly modular and segregated topology achieve best performances in simultaneous tasks with respect to random networks, despite random networks outperforming NW networks on independent tasks. Although no radical differences in RC computing performances were observed by considering the effect of NW stacking on the network topology and by considering physically realistic electrode configurations, Daniels *et al* [19] showed through simulations that quasi-3D (stacked) networks are more resilient to changes in input parameters allowing better generalization to noisy training data.

In contrast to most other studies that focus on exploring dynamics of self-assembled networks of nanoobjects for the realization of physical reservoirs while implementing in software the readout layer, Milano *et al* [15] experimentally demonstrated a fully memristive architecture for RC where both the reservoir and readout sections are implemented in hardware, as schematized in figure 8(c). In this case, a self-organizing NW network reservoir realized with a bottom-up approach was coupled with a memristive readout based on conventional ReRAM cells realized with a top-down approach. Here, readout classification was performed in hardware by means of a neural network realized with an array of ReRAMs, where matrix–vector multiplication was performed in one-shot through physical multiplication by Ohm's law and physical summation by Kirchhoff's law. Different implementation strategies of physical RC in NW networks have been explored in [207].

5.2. Generalization of the perceptron model and its physical implementation

Memristors have been proposed for the physical realization of the perceptron synaptic weights for ANN hardware [9, 140]. The use of memristors allows the physical encoding of these weights: the inputs superposition, i.e. computation, and their memory, that is the physical state of the system, are realized in the same hardware with substantial power reduction compared to standard digital components [9, 208].

Figure 8(a)) reports a scheme of the architecture based on a single perceptron as a binary classifier [11]: the weights associated with each input can be independently adjusted to give the desired output. Figure 8(b) shows a generalization of the model based on weights which are not related to a single input. A network of highly interconnected non-linear junctions resulting from the assembling of nanoparticle can dynamically change its connectivity and the topology of conducting pathways depending on the input stimuli, thus representing a suitable substrate for the scheme reported in figure 8(b) [121].

The weights $w_1, \ldots, w_n$ between any given pair of inputs and outputs depend on the overall response of the network to inputs $x_1, \ldots, x_n$. The weights are functions of a convolution of the input topology with the network conducting path topology resulting in the mapping of the weighted inputs $\Sigma' = x_1 w_1 (x_1, \ldots, x_n) + \ldots + x_n w_n (x_1, \ldots, x_n)$ to the output value $F(\Sigma')$. The perceptron thus represents the case where the weights are independent $w_1 (x_1, \ldots, x_n) = w_1, \ldots, w_n (x_1, \ldots, x_n) = w_n$.

Starting from the traditional perceptron model based on linearly independent weights:

$$S = \sum_{j=1}^{n} x_j w_j^P \quad (1)$$

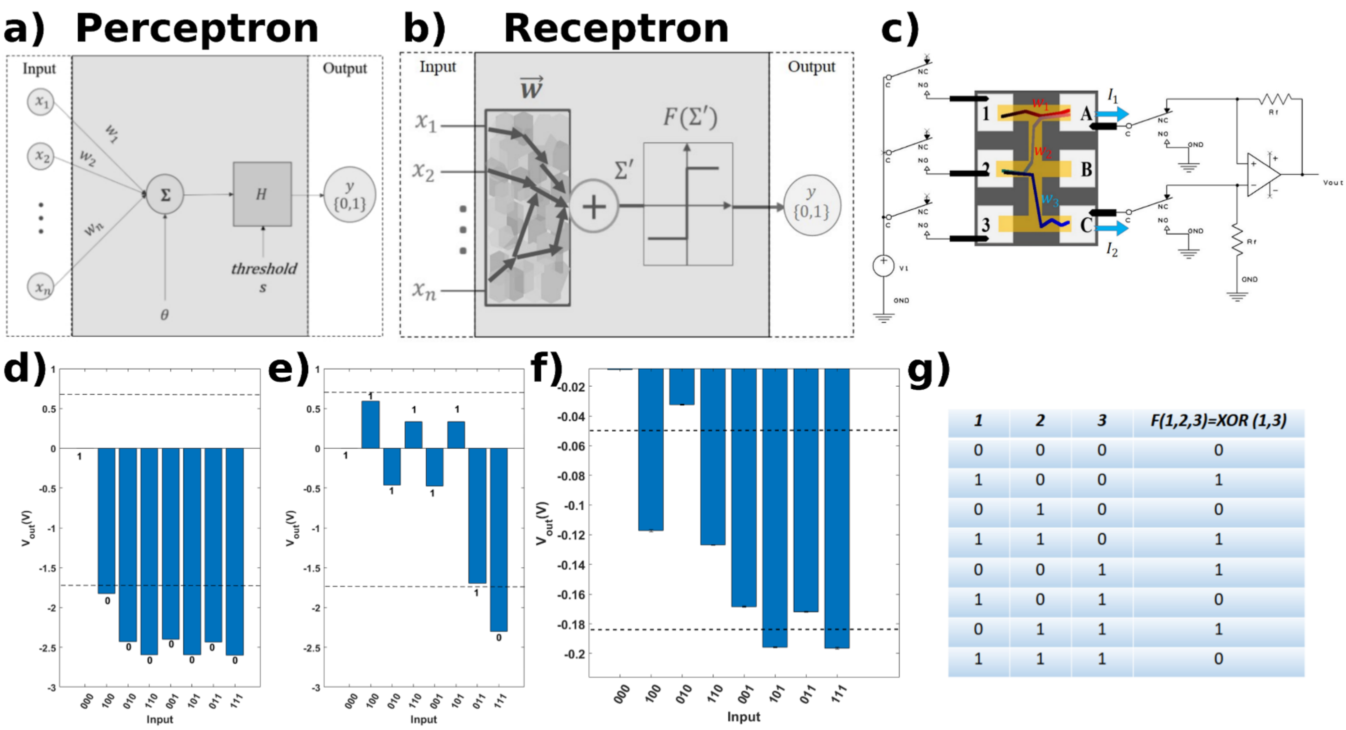

Figure 8. (a) Scheme of a perceptron. The inputs $x_1,\ldots,x_n$ are connected to the central unit through weighted links. (b) Scheme of an input-dependent and distributed weight device. The distributed weights $\vec{w} = (w_1,\ldots,w_N)$ are connected through a non-local and correlated weighting process on the signals coming from the inputs (rectangular area). (c) Circuital scheme of the 3-input receptron. Three input electrodes are shown (left), connected to relays that can be switched between voltage source and open circuit. The electrodes are connected to cluster-assembled film. Electrodes *A, B* and *C* are used as outputs (*B* is grounded). The outputs I_1 and I_2 result from the sum of the local currents flowing through the cluster-assembled film (color lines). (d)–(f) Examples of Boolean functions obtained imposing a two-threshold band on the measured voltage output. The dotted lines represent the two threshold values; the output voltage between the threshold provide a receptron state with logic value 1, while the output voltage outside the thresholds, provide the logic values 0. (d) NOR logic gate and (e) NAND logic gate for the same threshold band. (f) XOR logic gate; (g) truth table for the XOR function for inputs 1 and 3. Reproduced from [121]. © Mirigliano *et al* Published by IOP Publishing Ltd. CC BY 4.0.

where j numbers the inputs ($j \in [1,n]$) and w_j^P are constant real values, one can introduce a more general form of previous equation, which allows for the non-linear interaction of the inputs,

$$S = \sum_{j=1}^{n} x_j \tilde{w}_j(\vec{x}) \mid S \in R, \tag{2}$$

where $\tilde{w}_j(\vec{x}) : R^n \to C$ are complex-valued functions and $\vec{x} = (x_1,\ldots,x_n)$ is the input vector [209].

This is the basis of the receptron model: while equation (1) is a linear combination of the inputs (the weights are constant), in the receptron a modification of the inputs leads, in general, to a variation of the weights value $\tilde{w}_j(\vec{x})$ (equation (2)) introducing higher order non-linear terms in the sum thus making the system highly complex and allowing the classification of non-linearly separable functions with a single device using a single threshold, as described in detail in [205].

Figure 8(c) shows the scheme of a three input (3-bit) receptron fabricated by connecting with a nanostructured Au film three couple of electrodes [121]. Three relays connected to electrodes 1-2-3 can be switched between the voltage source or open circuit. Two relays connected to electrodes *A* and *C* can be switched between ground and, respectively, inverting and no-inverting input of an Op-Amp [121, 210].

To utilize a receptron as a binary classifier, one must first read an input signal, adjust the weights for each set of inputs, and then apply a thresholding procedure to the collected readings. This process generates a binary output that facilitates the execution of a classification task [11]. This leads to a protocol comprising two primary steps: the input reading step and the weight adjustment step (writing step). During the reading step, electrodes 1, 2, and 3 serve as the input electrodes (as shown in figure 8(c)), while electrodes *A* and *C* are connected to the operational amplifier (op-amp). The input logic 0 corresponds to a high impedance state (open relay in figure 8(c)), whereas the input logic 1 corresponds to a low impedance state (closed relay in figure 8(c)). The device output is the voltage V_{out} from the op-amp; by applying a threshold, a digital output is obtained. V_{out} can be measured for each input configuration, allowing for a complete definition of the Boolean device, which associates a binary value, derived from the thresholding process, with each input configuration (for example, 0-0-0, 1-0-0, etc). The thresholding process involves binarizing the voltage outputs through appropriate upper and lower thresholds. Output values falling within this specified range are linked to the logic value 1, while those outside yield a logic value of 0. The output function can be read multiple times since the reading process does not alter the weight distribution of the device (see figures 8(d)–(g)).

The modification of the weight distribution is obtained through the writing step: in this case electrodes 1,2 and 3 as input while A and C are grounded. A series of voltage pulses above a suitable threshold voltage can be applied to induce modification in the conduction path of the film (figure 8(c)).

Since the thresholding process imposed on the voltage output, together with the non-local effects of a writing process, limit the output explored by the device, a random search protocol could be advantageous to efficiently generate the desired Boolean functions, as in the case shown in figure 8(f), where the use of a double threshold improves the efficiency of the random search protocol.

A random search strategy has been proposed for neural network models based on the analogy with the immune system [211] and for hyperparameter optimization [212]. In the case where there is a very large number of configurations (current pathways, in this case) that can generate a favorable weight distribution, the random method seems to be better than the systematic one [17].

6. Conclusion and outlook

The integration of memristive crossbar arrays with transistor-based integrated circuits have demonstrated that different processes and devices can be successfully integrated to conventional microelectronics CMOS manufacturing [213]. In particular, a common pathway is to integrate memristive crossbar arrays after the metallization layers have been manufactured at the back-end-of-line to circuit logics [214].

The strategy for the fabrication of data processing systems based on self-assembled nanoobjects should be based on different approaches: the need for digital and analog devices coexisting on the same platform implies the integration of hardware with different length scale features and large material diversity [16, 215, 216]. This rapidly evolving scenario demands a paradigm shift towards the fabrication and characterization of hybrid systems where heterogeneous nanoscale materials must coexist and integrate with fabrication technologies typical of silicon [217, 218]. In particular, several critical factors need to be taken into account, including batch reproducibility, scalability, compatibility with planar technologies, parallel fabrication, and stability under harsh chemical and physical conditions [219]. While nanotechnology is considered to enable new production paradigms, the integration of various manufacturing processes is still hindered by the disparity in maturity levels between top-down and bottom-up approaches regarding production scalability, cost-effectiveness, reliability, and compliance with industrial and environmental standards [219, 220].

The standard top-down/bottom-up integration methods necessitate solutions capable of delivering and placing individual components at specific addressable locations on patterned surfaces. Therefore, a key challenge is the manipulation of nanoscale objects, such as nanoparticles or nanowires. Self-assembly strategies alleviate these demands, allowing for milder processing conditions, reduced contamination, and higher deposition rates [58]. The compatibility of the deposition process with a wide range of substrates and standard shadow masking techniques is also crucial [221, 222].

This represents a substantial departure from the paradigm of integrated microelectronic circuits, where every circuit element (e.g. transistor or memristive crossbar element) is meant to be addressed individually. However, to harness the functionality of emergent phenomena in nanostructured networks it is neither necessary nor meaningful to attempt to address every nanoobject in an extended nanogranular network individually [174]. In contrast, the whole network of nanoobjects can be addressed as a matrix of elements with given connections, e.g. for applications like RC [193].

Data availability statement

All data that support the findings of this study are included within the article (and any supplementary files).

Acknowledgments

A V acknowledges support from the Deutsche Forschungsgemeinschaft (DFG, German Research Foundation)—Project-ID 434434223—SFB 1461.

G M acknowledges partial support from the European project MEMQuD, code 20FUN06. This project (EMPIR 20FUN06 MEMQuD) has received funding from the EMPIR programme co-financed by the Participating States and from the European Union's Horizon 2020 research and innovation programme. Part of this work was financially supported by the Italian project NEURONE (Grant No. 20229JRTZA). The project received funding from the Italian programme for Research Projects of outstanding National Interest (PRIN) and Next Generation EU.

S A B acknowledges support from the Marsden Fund and the MacDiarmid Institute for Advanced Materials and Nanotechnology.

P M acknowledges support from the project MUSA—Multilayered Urban Sustainability Action—project, funded by the European Union—NextGenerationEU, under the National Recovery and Resilience Plan (NRRP) Mission 4 Component 2 Investment Line 1.5: Strenghtening of research structures and creation of R&D 'innovation ecosystems', set up of 'territorial leaders in R&D'. He also thanks M. Mirigliano and B. Paroli for discussions.

Conflict of interest

All authors declare no conflict of interest.

ORCID iDs

Alexander Vahl https://orcid.org/0000-0002-7311-272X
Gianluca Milano https://orcid.org/0000-0002-1983-6516
Zdenka Kuncic https://orcid.org/0000-0001-6765-3215
Simon A Brown https://orcid.org/0000-0002-6041-4331
Paolo Milani https://orcid.org/0000-0001-9325-4963

References

[1] Jaeger H 2021 Towards a generalized theory comprising digital, neuromorphic and unconventional computing *Neuromorph. Comput. Eng.* **1** 012002
[2] Sarkar T, Lieberth K, Pavlou A, Frank T, Mailaender V, McCulloch I, Blom P W M, Torricelli F and Gkoupidenis P 2022 An organic artificial spiking neuron for in situ neuromorphic sensing and biointerfacing *Nat. Electron.* **5** 774–83
[3] Ham D, Park H, Hwang S and Kim K 2021 Neuromorphic electronics based on copying and pasting the brain *Nat. Electron.* **4** 635–44
[4] Shannon C E, Sloane N J A and Wyner A D 1993 *Claude Elwood Shannon: Collected Papers* (IEEE Press)
[5] Von Neumann J 1956 Probabilistic logics and the synthesis of reliable organisms from unreliable components *Automata Studies. (AM-34)* ed C E Shannon and J McCarthy (Princeton University Press) pp 43–98
[6] Block H D, Knight B W and Rosenblatt F 1962 Analysis of a four-layer series-coupled perceptron. II *Rev. Mod. Phys.* **34** 135–42
[7] Minsky M 1961 Steps toward artificial intelligence *Proc. IRE* **49** 8–30
[8] LeCun Y, Bengio Y and Hinton G 2015 Deep learning *Nature* **521** 436–44
[9] Alibart F, Zamanidoost E and Strukov D B 2013 Pattern classification by memristive crossbar circuits using ex situ and in situ training *Nat. Commun.* **4** 2072
[10] Indiveri G and Liu S-C 2015 Memory and information processing in neuromorphic systems *Proc. IEEE* **103** 1379–97
[11] Minsky M and Papert S A 2017 *Perceptrons: An Introduction to Computational Geometry* (The MIT Press) (https://doi.org/10.7551/mitpress/11301.001.0001)
[12] Hopfield J J 1984 Neurons with graded response have collective computational properties like those of two-state neurons *Proc. Natl Acad. Sci. USA* **81** 3088–92
[13] Wang Z *et al* 2020 Resistive switching materials for information processing *Nat. Rev. Mater.* **5** 173–95
[14] Stepney S *et al* 2005 Journeys in non-classical computation I: a grand challenge for computing research *Int. J. Parallel Emergent Distrib. Syst.* **20** 5–19
[15] Milano G, Pedretti G, Montano K, Ricci S, Hashemkhani S, Boarino L, Ielmini D and Ricciardi C 2022 In materia reservoir computing with a fully memristive architecture based on self-organizing nanowire networks *Nat. Mater.* **21** 195–202
[16] Terasa M-I *et al* 2023 Pathways towards truly brain-like computing primitives *Mater. Today* **69** 41–53
[17] Turing A M 1950 Computing machinery and intelligence *Mind* **LIX** 433–60
[18] Milano G, Pedretti G, Fretto M, Boarino L, Benfenati F, Ielmini D, Valov I and Ricciardi C 2020 Brain-inspired structural plasticity through reweighting and rewiring in multi-terminal self-organizing memristive nanowire networks *Adv. Intell. Syst.* **2** 2000096
[19] Daniels R K, Mallinson J B, Heywood Z E, Bones P J, Arnold M D and Brown S A 2022 Reservoir computing with 3D nanowire networks *Neural Netw.* **154** 122–30
[20] Mallinson J B, Shirai S, Acharya S K, Bose S K, Galli E and Brown S A 2019 Avalanches and criticality in self-organized nanoscale networks *Sci. Adv.* **5** eaaw8438
[21] Mirigliano M, Decastri D, Pullia A, Dellasega D, Casu A, Falqui A and Milani P 2020 Complex electrical spiking activity in resistive switching nanostructured Au two-terminal devices *Nanotechnology* **31** 234001
[22] Sandouk E J, Gimzewski J K and Stieg A Z 2015 Multistate resistive switching in silver nanoparticle films *Sci. Technol. Adv. Mater.* **16** 045004
[23] Manning H G *et al* 2018 Emergence of winner-takes-all connectivity paths in random nanowire networks *Nat. Commun.* **9** 3219
[24] Diaz-Alvarez A, Higuchi R, Sanz-Leon P, Marcus I, Shingaya Y, Stieg A Z, Gimzewski J K, Kuncic Z and Nakayama T 2019 Emergent dynamics of neuromorphic nanowire networks *Sci. Rep.* **9** 14920
[25] Scharnhorst K S, Carbajal J P, Aguilera R C, Sandouk E J, Aono M, Stieg A Z and Gimzewski J K 2018 Atomic switch networks as complex adaptive systems *Jpn. J. Appl. Phys.* **57** 03ED02
[26] Sillin H O, Aguilera R, Shieh H-H, Avizienis A V, Aono M, Stieg A Z and Gimzewski J K 2013 A theoretical and experimental study of neuromorphic atomic switch networks for reservoir computing *Nanotechnology* **24** 384004
[27] Acharya S K, Galli E, Mallinson J B, Bose S K, Wagner F, Heywood Z E, Bones P J, Arnold M D and Brown S A 2021 Stochastic spiking behavior in neuromorphic networks enables true random number generation *ACS Appl. Mater. Interfaces* **13** 52861–70
[28] Carstens N, Adejube B, Strunskus T, Faupel F, Brown S and Vahl A 2022 Brain-like critical dynamics and long-range temporal correlations in percolating networks of silver nanoparticles and functionality preservation after integration of insulating matrix *Nanoscale Adv.* **4** 3149–60
[29] Stieg A Z, Avizienis A V, Sillin H O, Martin-Olmos C, Aono M and Gimzewski J K 2012 Emergent criticality in complex turing B-type atomic switch networks *Adv. Mater.* **24** 286–93
[30] Avizienis A V, Sillin H O, Martin-Olmos C, Shieh H H, Aono M, Stieg A Z and Gimzewski J K 2012 Neuromorphic atomic switch networks *PLoS One* **7** e42772
[31] Palmigiano A, Geisel T, Wolf F and Battaglia D 2017 Flexible information routing by transient synchrony *Nat. Neurosci.* **20** 1014–22
[32] DeBenedictis E P, Badaroglu M, Chen A, Conte T M and Gargini P 2017 Sustaining Moore's law with 3D chips *Computer* **50** 69–73
[33] Ielmini D, Cagli C, Nardi F and Zhang Y 2013 Nanowire-based resistive switching memories: devices, operation and scaling *J. Phys. D: Appl. Phys.* **46** 074006
[34] Gupta A, Wang Y and Markram H 2000 *Principles of Neural Science* (McGraw-Hill, Health Professions Division)
[35] Kurnia F, Liu C, Raveendra N, Jung C U, Vasudevan R K and Valanoor N 2020 Self-assembled NiO nanocrystal arrays as memristive elements *Adv. Electron. Mater.* **6** 1901153
[36] Vahl A, Carstens N, Strunskus T, Faupel F and Hassanien A 2019 Diffusive memristive switching on the nanoscale, from individual nanoparticles towards scalable nanocomposite devices *Sci. Rep.* **9** 17367
[37] Carstens N, Strunskus T, Faupel F, Hassanien A and Vahl A 2023 Neuronal-like irregular spiking dynamics in highly volatile memristive intermediate-scale AgPt-nanoparticle assemblies *Part. Part. Syst. Charact.* **40** 2200131

[38] Yan X *et al* 2019 Self-assembled networked PbS distribution quantum dots for resistive switching and artificial synapse performance boost of memristors *Adv. Mater.* **31** 1805284
[39] You B K, Kim J M, Joe D J, Yang K, Shin Y, Jung Y S and Lee K J 2016 Reliable memristive switching memory devices enabled by densely packed silver nanocone arrays as electric-field concentrators *ACS Nano* **10** 9478–88
[40] You B K, Park W I, Kim J M, Park K-I, Seo H K, Lee J Y, Jung Y S and Lee K J 2014 Reliable control of filament formation in resistive memories by self-assembled nanoinsulators derived from a block copolymer *ACS Nano* **8** 9492–502
[41] Milani P and Sowwan M (eds) 2020 *Cluster Beam Deposition of Functional Nanomaterials and Devices* (Elsevier)
[42] Gronenberg O *et al* 2024 In situ imaging of dynamic current paths in a neuromorphic nanoparticle network with critical spiking behavior *Adv. Funct. Mater.* **34** 2312989
[43] Bose S K, Lawrence C P, Liu Z, Makarenko K S, van Damme R M J, Broersma H J and van der Wiel W G 2015 Evolution of a designless nanoparticle network into reconfigurable Boolean logic *Nat. Nanotech.* **10** 1048–52
[44] Milano G, Miranda E and Ricciardi C 2022 Connectome of memristive nanowire networks through graph theory *Neural Netw.* **150** 137–48
[45] Terasa M-I, Holtz P, Carstens N, Kaps S, Faupel F, Vahl A and Adelung R 2022 Sparse CNT networks with implanted AgAu nanoparticles: a novel memristor with short-term memory bordering between diffusive and bipolar switching *PLoS One* **17** e0264846
[46] Milani P and Iannotta S 1999 *Cluster Beam Synthesis of Nanostructured Materials* (Springer) (https://doi.org/10.1007/978-3-642-59899-9)
[47] Wegner K, Piseri P, Tafreshi H V and Milani P 2006 Cluster beam deposition: a tool for nanoscale science and technology *J. Phys. D: Appl. Phys.* **39** R439–59
[48] Piseri P, Tafreshi H V and Milani P 2004 Manipulation of nanoparticles in supersonic beams for the production of nanostructured materials *Curr. Opin. Solid State Mater. Sci.* **8** 195–202
[49] Reichel R, Partridge J G, Dunbar A D F, Brown S A, Caughley O and Ayesh A 2006 Construction and application of a UHV compatible cluster deposition system *J. Nanopart. Res.* **8** 405–16
[50] Borghi F, Podestà A, Piazzoni C and Milani P 2018 Growth mechanism of cluster-assembled surfaces: from submonolayer to thin-film regime *Phys. Rev. Appl.* **9** 044016
[51] Podestà A, Bongiorno G, Scopelliti P E, Bovio S, Milani P, Semprebon C and Mistura G 2009 Cluster-assembled nanostructured titanium oxide films with tailored wettability *J. Phys. Chem.* C **113** 18264–9
[52] Podestà A, Borghi F, Indrieri M, Bovio S, Piazzoni C and Milani P 2015 Nanomanufacturing of titania interfaces with controlled structural and functional properties by supersonic cluster beam deposition *J. Appl. Phys.* **118** 234309
[53] Mirigliano M and Milani P 2021 Electrical conduction in nanogranular cluster-assembled metallic films *Adv. Phys.* X **6** 1908847
[54] Huttel Y (ed) 2017 *Gas-Phase Synthesis of Nanoparticles* (Wiley) (https://doi.org/10.1002/9783527698417)
[55] Santaniello T and Milani P 2020 Additive nano-manufacturing of 3D printed electronics using supersonic cluster beam deposition *Front. Nanosci.* **15** 313–33
[56] Barborini E, Piseri P and Milani P 1999 A pulsed microplasma source of high intensity supersonic carbon cluster beams *J. Phys. D: Appl. Phys.* **32** L105–9
[57] Piseri P, Podestà A, Barborini E and Milani P 2001 Production and characterization of highly intense and collimated cluster beams by inertial focusing in supersonic expansions *Rev. Sci. Instrum.* **72** 2261–7
[58] Barborini E *et al* 2008 Batch fabrication of metal oxide sensors on micro-hotplates *J. Micromech. Microeng.* **18** 055015
[59] Marelli M, Divitini G, Collini C, Ravagnan L, Corbelli G, Ghisleri C, Gianfelice A, Lenardi C, Milani P and Lorenzelli L 2011 Flexible and biocompatible microelectrode arrays fabricated by supersonic cluster beam deposition on SU-8 *J. Micromech. Microeng.* **21** 045013
[60] Bose S K, Mallinson J B, Gazoni R M and Brown S A 2017 Stable self-assembled atomic-switch networks for neuromorphic applications *IEEE Trans. Electron. Devices* **64** 5194–201
[61] Sattar A, Fostner S and Brown S A 2013 Quantized conductance and switching in percolating nanoparticle films *Phys. Rev. Lett.* **111** 136808
[62] Drewes J, Vahl A, Carstens N, Strunskus T, Polonskyi O and Faupel F 2021 Enhancing composition control of alloy nanoparticles from gas aggregation source by in operando optical emission spectroscopy *Plasma Process. Polym.* **18** 2000208
[63] Vahl A, Strobel J, Reichstein W, Polonskyi O, Strunskus T, Kienle L and Faupel F 2017 Single target sputter deposition of alloy nanoparticles with adjustable composition via a gas aggregation cluster source *Nanotechnology* **28** 175703
[64] Nikitin D *et al* 2023 Resistive switching effect in Ag-poly(ethylene glycol) nanofluids: novel avenue toward neuromorphic materials *Adv. Funct. Mater.* **34** 2310473
[65] Wang J, Choudhary S, Harrigan W L, Crosby A J, Kittilstved K R and Nonnenmann S S 2017 Transferable memristive nanoribbons comprising solution-processed strontium titanate nanocubes *ACS Appl. Mater. Interfaces* **9** 10847–54
[66] Zhou Z *et al* 2021 Memristive behavior of mixed oxide nanocrystal assemblies *ACS Appl. Mater. Interfaces* **13** 21635–44
[67] Milano G, Porro S, Valov I and Ricciardi C 2019 Recent developments and perspectives for memristive devices based on metal oxide nanowires *Adv. Electron. Mater.* **5** 1800909
[68] Nirmalraj P N *et al* 2012 Manipulating connectivity and electrical conductivity in metallic nanowire networks *Nano Lett.* **12** 5966–71
[69] Demis E C, Aguilera R, Sillin H O, Scharnhorst K, Sandouk E J, Aono M, Stieg A Z and Gimzewski J K 2015 Atomic switch networks—nanoarchitectonic design of a complex system for natural computing *Nanotechnology* **26** 204003
[70] Burr G W *et al* 2017 Neuromorphic computing using non-volatile memory *Adv. Phys.* X **2** 89–124
[71] Kendall J D and Kumar S 2020 The building blocks of a brain-inspired computer *Appl. Phys. Rev.* **7** 011305
[72] Zidan M A, Strachan J P and Lu W D 2018 The future of electronics based on memristive systems *Nat. Electron.* **1** 22–29
[73] Duan X, Cao Z, Gao K, Yan W, Sun S, Zhou G, Wu Z, Ren F and Sun B 2024 Memristor-based neuromorphic chips *Adv. Mater.* **36** 2310704
[74] Waser R and Aono M 2007 Nanoionics-based resistive switching memories *Nat. Mater.* **6** 833–40
[75] Nishioka D, Tsuchiya T, Namiki W, Takayanagi M, Imura M, Koide Y, Higuchi T and Terabe K 2022 Edge-of-chaos learning achieved by ion-electron–coupled dynamics in an ion-gating reservoir *Sci. Adv.* **8** eade1156

[76] Valov I, Waser R, Jameson J R and Kozicki M N 2011 Electrochemical metallization memories—fundamentals, applications, prospects *Nanotechnology* **22** 289502

[77] Loeffler A, Zhu R, Hochstetter J, Li M, Fu K, Diaz-Alvarez A, Nakayama T, Shine J M and Kuncic Z 2020 Topological properties of neuromorphic nanowire networks *Front. Neurosci.* **14** 184

[78] Shirai S, Acharya S K, Bose S K, Mallinson J B, Galli E, Pike M D, Arnold M D and Brown S A 2020 Long-range temporal correlations in scale-free neuromorphic networks *Netw. Neurosci.* **4** 432–47

[79] Daniels R K, Arnold M D, Heywood Z E, Mallinson J B, Bones P J and Brown S A 2023 Brainlike networks of nanowires and nanoparticles: a change of perspective *Phys. Rev. Appl.* **20** 034021

[80] Milano G, Luebben M, Ma Z, Dunin-Borkowski R, Boarino L, Pirri C F, Waser R, Ricciardi C and Valov I 2018 Self-limited single nanowire systems combining all-in-one memristive and neuromorphic functionalities *Nat. Commun.* **9** 5151

[81] Wang Z *et al* 2017 Memristors with diffusive dynamics as synaptic emulators for neuromorphic computing *Nat. Mater.* **16** 101–8

[82] Valov I and Lu W D 2016 Nanoscale electrochemistry using dielectric thin films as solid electrolytes *Nanoscale* **8** 13828–37

[83] Yang Y, Gao P, Li L, Pan X, Tappertzhofen S, Choi S, Waser R, Valov I and Lu W D 2014 Electrochemical dynamics of nanoscale metallic inclusions in dielectrics *Nat. Commun.* **5** 4232

[84] Milano G, Porro S, Ali M Y, Bejtka K, Bianco S, Beccaria F, Chiolerio A, Pirri C F and Ricciardi C 2018 Unravelling resistive switching mechanism in ZnO NW arrays: the role of the polycrystalline base layer *J. Phys. Chem.* C **122** 866–74

[85] Kim S I, Lee J H, Chang Y W, Hwang S S and Yoo K-H 2008 Reversible resistive switching behaviors in NiO nanowires *Appl. Phys. Lett.* **93** 033503

[86] Huang C-H, Chou T-S, Huang J-S, Lin S-M and Chueh Y-L 2017 Self-selecting resistive switching scheme using TiO_2 nanorod arrays *Sci. Rep.* **7** 2066

[87] Porro S, Risplendi F, Cicero G, Bejtka K, Milano G, Rivolo P, Jasmin A, Chiolerio A, Pirri C F and Ricciardi C 2017 Multiple resistive switching in core–shell ZnO nanowires exhibiting tunable surface states *J. Mater. Chem.* C **5** 10517–23

[88] Chang W-Y, Lin C-A, He J-H and Wu T-B 2010 Resistive switching behaviors of ZnO nanorod layers *Appl. Phys. Lett.* **96** 242109

[89] Fra V, Beccaria M, Milano G, Guastella S, Bianco S, Porro S, Laurenti M, Stassi S and Ricciardi C 2020 Hydrothermally grown ZnO nanowire array as an oxygen vacancies reservoir for improved resistive switching *Nanotechnology* **31** 374001

[90] Milano G, Boarino L and Ricciardi C 2019 Junction properties of single ZnO nanowires with asymmetrical Pt and Cu contacts *Nanotechnology* **30** 244001

[91] Nagashima K, Yanagida T, Oka K, Kanai M, Klamchuen A, Kim J-S, Park B H and Kawai T 2011 Intrinsic mechanisms of memristive switching *Nano Lett.* **11** 2114–8

[92] Nagashima K, Yanagida T, Oka K, Taniguchi M, Kawai T, Kim J-S and Park B H 2010 Resistive switching multistate nonvolatile memory effects in a single cobalt oxide nanowire *Nano Lett.* **10** 1359–63

[93] Oka K, Yanagida T, Nagashima K, Kanai M, Kawai T, Kim J-S and Park B H 2011 Spatial nonuniformity in resistive-switching memory effects of NiO *J. Am. Chem. Soc.* **133** 12482–5

[94] Milano G, Raffone F, Luebben M, Boarino L, Cicero G, Valov I and Ricciardi C 2020 Water-mediated ionic migration in memristive nanowires with a tunable resistive switching mechanism *ACS Appl. Mater. Interfaces* **12** 48773–80

[95] Hong D S, Chen Y S, Sun J R and Shen B G 2016 Ternary synaptic plasticity arising from memdiode behavior of TiO_x single nanowires *Adv. Electron. Mater.* **2** 1500359

[96] Milano G, Miranda E, Fretto M, Valov I and Ricciardi C 2022 Experimental and modeling study of metal–insulator interfaces to control the electronic transport in single nanowire memristive devices *ACS Appl. Mater. Interfaces* **14** 53027–37

[97] Milano G, Raffone F, Bejtka K, De Carlo I, Fretto M, Pirri F C, Cicero G, Ricciardi C and Valov I 2024 Electrochemical rewiring through quantum conductance effects in single metallic memristive nanowires *Nanoscale Horiz.* **9** 416–26

[98] Milano G, Luebben M, Laurenti M, Porro S, Bejtka K, Bianco S, Breuer U, Boarino L, Valov I and Ricciardi C 2019 Ionic modulation of electrical conductivity of ZnO due to ambient moisture *Adv Mater. Interfaces* **6** 1900803

[99] Milano G, Boarino L, Valov I and Ricciardi C 2022 Memristive devices based on single ZnO nanowires—from material synthesis to neuromorphic functionalities *Semicond. Sci. Technol.* **37** 034002

[100] Song M-K *et al* 2023 Recent advances and future prospects for memristive materials, devices, and systems *ACS Nano* **17** 11994–2039

[101] Tang J *et al* 2019 Bridging biological and artificial neural networks with emerging neuromorphic devices: fundamentals, progress, and challenges *Adv. Mater.* **31** 1902761

[102] Xia Q and Yang J J 2019 Memristive crossbar arrays for brain-inspired computing *Nat. Mater.* **18** 309–23

[103] Zhang Y *et al* 2020 Brain-inspired computing with memristors: challenges in devices, circuits, and systems *Appl. Phys. Rev.* **7** 011308

[104] Valov I, Linn E, Tappertzhofen S, Schmelzer S, van den Hurk J, Lentz F and Waser R 2013 Nanobatteries in redox-based resistive switches require extension of memristor theory *Nat. Commun.* **4** 1771

[105] Wang W, Wang M, Ambrosi E, Bricalli A, Laudato M, Sun Z, Chen X and Ielmini D 2019 Surface diffusion-limited lifetime of silver and copper nanofilaments in resistive switching devices *Nat. Commun.* **10** 81

[106] Pike M D, Bose S K, Mallinson J B, Acharya S K, Shirai S, Galli E, Weddell S J, Bones P J, Arnold M D and Brown S A 2020 Atomic scale dynamics drive brain-like avalanches in percolating nanostructured networks *Nano Lett.* **20** 3935–42

[107] Kim Y, An J S, Lee D, Ryu S Y, Hwang Y-C, Kim D H and Kim T W 2023 Biocompatible memristive device based on an agarose@gold nanoparticle-nanocomposite layer obtained from nature for neuromorphic computing *Sci. Rep.* **13** 6491

[108] Zabet-Khosousi A, Trudeau P-E, Suganuma Y, Dhirani A-A and Statt B 2006 Metal to insulator transition in films of molecularly linked gold nanoparticles *Phys. Rev. Lett.* **96** 156403

[109] Kirkpatrick S 1973 Percolation and conduction *Rev. Mod. Phys.* **45** 574–88

[110] Fostner S, Brown R, Carr J and Brown S A 2014 Continuum percolation with tunneling *Phys. Rev.* B **89** 075402

[111] Mirigliano M, Borghi F, Podestà A, Antidormi A, Colombo L and Milani P 2019 Non-ohmic behavior and resistive switching of Au cluster-assembled films beyond the percolation threshold *Nanoscale Adv.* **1** 3119–30

[112] Mirigliano M, Radice S, Falqui A, Casu A, Cavaliere F and Milani P 2020 Anomalous electrical conduction and negative temperature coefficient of resistance in nanostructured gold resistive switching films *Sci. Rep.* **10** 19613

[113] Minnai C, Bellacicca A, Brown S A and Milani P 2017 Facile fabrication of complex networks of memristive devices *Sci. Rep.* **7** 7955

[114] Barborini E, Corbelli G, Bertolini G, Repetto P, Leccardi M, Vinati S and Milani P 2010 The influence of nanoscale morphology on the resistivity of cluster-assembled nanostructured metallic thin films *New J. Phys.* **12** 073001

[115] Borghi F, Mirigliano M, Dellasega D and Milani P 2022 Influence of the nanostructure on the electric transport properties of resistive switching cluster-assembled gold films *Appl. Surf. Sci.* **582** 152485

[116] Kim T-H, Zhang X-G, Nicholson D M, Evans B M, Kulkarni N S, Radhakrishnan B, Kenik E A and Li A-P 2010 Large discrete resistance jump at grain boundary in copper nanowire *Nano Lett.* **10** 3096–100

[117] Tarantino W and Colombo L 2020 Modeling resistive switching in nanogranular metal films *Phys. Rev. Res.* **2** 043389

[118] Halbritter A, Csonka S, Kolesnychenko O Y, Mihály G, Shklyarevskii O I and van Kempen H 2002 Connective neck evolution and conductance steps in hot point contacts *Phys. Rev.* B **65** 045413

[119] Buffat P and Borel J-P 1976 Size effect on the melting temperature of gold particles *Phys. Rev.* A **13** 2287–98

[120] Iijima S and Ichihashi T 1986 Structural instability of ultrafine particles of metals *Phys. Rev. Lett.* **56** 616–9

[121] Mirigliano M, Paroli B, Martini G, Fedrizzi M, Falqui A, Casu A and Milani P 2021 A binary classifier based on a reconfigurable dense network of metallic nanojunctions *Neuromorph. Comput. Eng.* **1** 024007

[122] Breakspear M 2017 Dynamic models of large-scale brain activity *Nat. Neurosci.* **20** 340–52

[123] Hochstetter J, Zhu R, Loeffler A, Diaz-Alvarez A, Nakayama T and Kuncic Z 2021 Avalanches and edge-of-chaos learning in neuromorphic nanowire networks *Nat. Commun.* **12** 4008

[124] Hoshino O, Kashimori Y and Kambara T 1996 Self-organized phase transitions in neural networks as a neural mechanism of information processing *Proc. Natl Acad. Sci. USA* **93** 3303–7

[125] Levina A, Herrmann J M and Geisel T 2009 Phase transitions towards criticality in a neural system with adaptive interactions *Phys. Rev. Lett.* **102** 118110

[126] Faupel F, Zaporojtchenko V, Strunskus T and Elbahri M 2010 Metal-polymer nanocomposites for functional applications *Adv. Eng. Mater.* **12** 1177–90

[127] Melinon P, Jensen P, Hu J X, Hoareau A, Cabaud B, Treilleux M and Guillot D 1991 Comparison of molecular and cluster deposition: evidence of different percolation processes *Phys. Rev.* B **44** 12562–4

[128] Schmelzer J, Brown S A, Wurl A, Hyslop M and Blaikie R J 2002 Finite-size effects in the conductivity of cluster assembled nanostructures *Phys. Rev. Lett.* **88** 226802

[129] Bose S K, Mallinson J B, Galli E, Acharya S K, Minnai C, Bones P J and Brown S A 2022 Neuromorphic behaviour in discontinuous metal films *Nanoscale Horiz.* **7** 437–45

[130] Stauffer D and Aharony A 2018 *Introduction to Percolation Theory* (Taylor & Francis) (https://doi.org/10.1201/9781315274386)

[131] Dunbar A D F, Partridge J G, Schulze M and Brown S A 2006 Morphological differences between Bi, Ag and Sb nano-particles and how they affect the percolation of current through nano-particle networks *Eur. Phys. J.* D **39** 415–22

[132] Ayesh A I, Brown S A, Awasthi A, Hendy S C, Convers P Y and Nichol K 2010 Coefficient of restitution for bouncing nanoparticles *Phys. Rev.* B **81** 195422

[133] Awasthi A, Hendy S C, Zoontjens P and Brown S A 2006 Reentrant adhesion behavior in nanocluster deposition *Phys. Rev. Lett.* **97** 186103

[134] Awasthi A, Hendy S C, Zoontjens P, Brown S A and Natali F 2007 Molecular dynamics simulations of reflection and adhesion behavior in Lennard-Jones cluster deposition *Phys. Rev.* B **76** 115437

[135] Reichel R *et al* 2006 From the adhesion of atomic clusters to the fabrication of nanodevices *Appl. Phys. Lett.* **89** 213105

[136] Partridge J G, Brown S A, Dunbar A D F, Reichel R, Kaufmann M, Siegert C, Scott S and Blaikie R J 2004 Templated-assembly of conducting antimony cluster wires *Nanotechnology* **15** 1382–7

[137] Partridge J G, Scott S, Dunbar A D F, Schulze M, Brown S A, Wurl A and Blaikie R J 2004 Formation of electrically conducting mesoscale wires through self-assembly of atomic clusters *IEEE Trans. Nanotechnol.* **3** 61–66

[138] Jensen P 1999 Growth of nanostructures by cluster deposition: experiments and simple models *Rev. Mod. Phys.* **71** 1695–735

[139] Schulze M *et al* 2003 Electrical measurements of nanoscale bismuth cluster films *Eur. Phys. J.* D **24** 291–4

[140] Strukov D B, Snider G S, Stewart D R and Williams R S 2008 The missing memristor found *Nature* **453** 80–83

[141] Balberg I, Azulay D, Toker D and Millo O 2004 Percolation and tunneling in composite materials *Int. J. Mod. Phys.* B **18** 2091–121

[142] Grimaldi C 2014 Theory of percolation and tunneling regimes in nanogranular metal films *Phys. Rev.* B **89** 214201

[143] Fostner S and Brown S A 2015 Neuromorphic behavior in percolating nanoparticle films *Phys. Rev.* E **92** 052134

[144] Li Y, Wang Z, Midya R, Xia Q and Yang J J 2018 Review of memristor devices in neuromorphic computing: materials sciences and device challenges *J. Phys. D: Appl. Phys.* **51** 503002

[145] Bose S K, Shirai S, Mallinson J B and Brown S A 2019 Synaptic dynamics in complex self-assembled nanoparticle networks *Faraday Discuss.* **213** 471–85

[146] Friedman N, Ito S, Brinkman B A W, Shimono M, DeVille R E L, Dahmen K A, Beggs J M and Butler T C 2012 Universal critical dynamics in high resolution neuronal avalanche data *Phys. Rev. Lett.* **108** 208102

[147] Sethna J P, Dahmen K A and Myers C R 2001 Crackling noise *Nature* **410** 242–50

[148] Tian Y, Tan Z, Hou H, Li G, Cheng A, Qiu Y, Weng K, Chen C and Sun P 2022 Theoretical foundations of studying criticality in the brain *Netw. Neurosci.* **6** 1148–85

[149] Cocchi L, Gollo L L, Zalesky A and Breakspear M 2017 Criticality in the brain: a synthesis of neurobiology, models and cognition *Prog. Neurobiol.* **158** 132–52

[150] Hesse J and Gross T 2014 Self-organized criticality as a fundamental property of neural systems *Front. Syst. Neurosci.* **8** 166

[151] Beggs J M and Plenz D 2003 Neuronal avalanches in neocortical circuits *J. Neurosci.* **23** 11167–77

[152] Chialvo D R 2010 Emergent complex neural dynamics *Nat. Phys.* **6** 744–50

[153] Shew W L, Yang H, Petermann T, Roy R and Plenz D 2009 Neuronal avalanches imply maximum dynamic range in cortical networks at criticality *J. Neurosci.* **29** 15595–600

[154] Muñoz M A 2018 *Colloquium*: criticality and dynamical scaling in living systems *Rev. Mod. Phys.* **90** 031001

[155] Srinivasa N, Stepp N D and Cruz-Albrecht J 2015 Criticality as a set-point for adaptive behavior in neuromorphic hardware *Front. Neurosci.* **9** 449

[156] Shew W L and Plenz D 2013 The functional benefits of criticality in the cortex *Neuroscientist* **19** 88–100
[157] Studholme S J, Heywood Z E, Mallinson J B, Steel J K, Bones P J, Arnold M D and Brown S A 2023 Computation via neuron-like spiking in percolating networks of nanoparticles *Nano Lett.* **23** 10594–9
[158] Daniels R K and Brown S A 2021 Nanowire networks: how does small-world character evolve with dimensionality? *Nanoscale Horiz.* **6** 482–8
[159] Heywood Z, Mallinson J, Galli E, Acharya S, Bose S, Arnold M, Bones P and Brown S 2022 Self-organized nanoscale networks: are neuromorphic properties conserved in realistic device geometries? *Neuromorph. Comput. Eng.* **2** 024009
[160] Carboni R and Ielmini D 2019 Stochastic memory devices for security and computing *Adv. Electron. Mater.* **5** 1900198
[161] Mazzoni A, Broccard F D, Garcia-Perez E, Bonifazi P, Ruaro M E and Torre V 2007 On the dynamics of the spontaneous activity in neuronal networks *PLoS One* **2** e439
[162] Hoffmann-Vogel R 2017 Electromigration and the structure of metallic nanocontacts *Appl. Phys. Rev.* **4** 031302
[163] Demis E C, Aguilera R, Scharnhorst K, Aono M, Stieg A Z and Gimzewski J K 2016 Nanoarchitectonic atomic switch networks for unconventional computing *Jpn. J. Appl. Phys.* **55** 1102B2
[164] Akai-Kasaya M, Takeshima Y, Kan S, Nakajima K, Oya T and Asai T 2022 Performance of reservoir computing in a random network of single-walled carbon nanotubes complexed with polyoxometalate *Neuromorph. Comput. Eng.* **2** 014003
[165] Fu K *et al* 2020 Reservoir computing with neuromemristive nanowire networks *2020 Int. Joint Conf. on Neural Networks (IJCNN)* (IEEE) pp 1–8
[166] Lilak S, Woods W, Scharnhorst K, Dunham C, Teuscher C, Stieg A Z and Gimzewski J K 2021 Spoken digit classification by in-materio reservoir computing with neuromorphic atomic switch networks *Front. Nanotechnol.* **3** 675792
[167] Loeffler A, Diaz-Alvarez A, Zhu R, Ganesh N, Shine J M, Nakayama T and Kuncic Z 2023 Neuromorphic learning, working memory, and metaplasticity in nanowire networks *Sci. Adv.* **9** eadg3289
[168] Strogatz S H 2001 Exploring complex networks *Nature* **410** 268–76
[169] Kuncic Z and Nakayama T 2021 Neuromorphic nanowire networks: principles, progress and future prospects for neuro-inspired information processing *Adv. Phys.* X **6** 1894234
[170] Dunham C S, Lilak S, Hochstetter J, Loeffler A, Zhu R, Chase C, Stieg A Z, Kuncic Z and Gimzewski J K 2021 Nanoscale neuromorphic networks and criticality: a perspective *J. Phys. Complex.* **2** 042001
[171] Khona M and Fiete I R 2022 Attractor and integrator networks in the brain *Nat. Rev. Neurosci.* **23** 744–66
[172] Beggs J M and Timme N 2012 Being critical of criticality in the brain *Front. Physiol.* **3** 163
[173] Plenz D, Ribeiro T L, Miller S R, Kells P A, Vakili A and Capek E L 2021 Self-organized criticality in the brain *Front. Phys.* **9** 639389
[174] Li Q, Diaz-Alvarez A, Iguchi R, Hochstetter J, Loeffler A, Zhu R, Shingaya Y, Kuncic Z, Uchida K-I and Nakayama T 2020 Dynamic electrical pathway tuning in neuromorphic nanowire networks *Adv. Funct. Mater.* **30** 2003679
[175] Milano G, Cultrera A, Boarino L, Callegaro L and Ricciardi C 2023 Tomography of memory engrams in self-organizing nanowire connectomes *Nat. Commun.* **14** 5723
[176] Cultrera A, Milano G, De Leo N, Ricciardi C, Boarino L and Callegaro L 2021 Recommended implementation of electrical resistance tomography for conductivity mapping of metallic nanowire networks using voltage excitation *Sci. Rep.* **11** 13167
[177] Milano G, Cultrera A, Bejtka K, De Leo N, Callegaro L, Ricciardi C and Boarino L 2020 Mapping time-dependent conductivity of metallic nanowire networks by electrical resistance tomography toward transparent conductive materials *ACS Appl. Nano Mater.* **3** 11987–97
[178] Montano K, Milano G and Ricciardi C 2022 Grid-graph modeling of emergent neuromorphic dynamics and heterosynaptic plasticity in memristive nanonetworks *Neuromorph. Comput. Eng.* **2** 014007
[179] Miranda E, Milano G and Ricciardi C 2020 Modeling of short-term synaptic plasticity effects in ZnO nanowire-based memristors using a potentiation-depression rate balance equation *IEEE Trans. Nanotechnol.* **19** 609–12
[180] Caravelli F, Sheldon F C and Traversa F L 2021 Global minimization via classical tunneling assisted by collective force field formation *Sci. Adv.* **7** eabh1542
[181] Caravelli F, Milano G, Ricciardi C and Kuncic Z 2023 Mean field theory of self-organizing memristive connectomes *Ann. Phys., Lpz.* **535** 2300090
[182] Zhu R, Hochstetter J, Loeffler A, Diaz-Alvarez A, Nakayama T, Lizier J T and Kuncic Z 2021 Information dynamics in neuromorphic nanowire networks *Sci. Rep.* **11** 13047
[183] Sheldon F C and Di Ventra M 2017 Conducting-insulating transition in adiabatic memristive networks *Phys. Rev.* E **95** 012305
[184] Hopfield J J 1982 Neural networks and physical systems with emergent collective computational abilities *Proc. NatL Acad. Sci. USA* **79** 2554–8
[185] Jaeger H and Haas H 2004 Harnessing nonlinearity: predicting chaotic systems and saving energy in wireless communication *Science* **304** 78–80
[186] Maass W 2011 Liquid state machines: motivation, theory, and applications *Computability in Context* (IMPERIAL COLLEGE PRESS) pp 275–96
[187] Nakajima K 2020 Physical reservoir computing—an introductory perspective *Jpn. J. Appl. Phys.* **59** 060501
[188] Tanaka G, Yamane T, Héroux J B, Nakane R, Kanazawa N, Takeda S, Numata H, Nakano D and Hirose A 2019 Recent advances in physical reservoir computing: a review *Neural Netw.* **115** 100–23
[189] Du C, Cai F, Zidan M A, Ma W, Lee S H and Lu W D 2017 Reservoir computing using dynamic memristors for temporal information processing *Nat. Commun.* **8** 2204
[190] Moon J, Ma W, Shin J H, Cai F, Du C, Lee S H and Lu W D 2019 Temporal data classification and forecasting using a memristor-based reservoir computing system *Nat. Electron.* **2** 480–7
[191] Dale M, Miller J F, Stepney S and Trefzer M A 2016 Evolving carbon nanotube reservoir computers *Unconventional Computation and Natural Computation* vol 9726, ed M Amos and A Condon (Springer International Publishing) pp 49–61
[192] Tanaka H *et al* 2022 In-materio computing in random networks of carbon nanotubes complexed with chemically dynamic molecules: a review *Neuromorph. Comput. Eng.* **2** 022002
[193] Zhu R, Lilak S, Loeffler A, Lizier J, Stieg A, Gimzewski J and Kuncic Z 2023 Online dynamical learning and sequence memory with neuromorphic nanowire networks *Nat. Commun.* **14** 6697
[194] Milano G, Agliuzza M, De Leo N and Ricciardi C 2022 Speech recognition through physical reservoir computing

with neuromorphic nanowire networks *2022 International Joint Conf. on Neural Networks (IJCNN)* (IEEE) pp 1–6

[195] Milano G, Chakrabarty T and Ricciardi C 2023 Mackey-glass time series forecasting by nanowire networks *2023 IEEE Int. Conf. on Metrology for eXtended Reality, Artificial Intelligence and Neural Engineering (MetroXRAINE)* (IEEE) pp 989–94

[196] Mallinson J B, Heywood Z E, Daniels R K, Arnold M D, Bones P J and Brown S A 2023 Reservoir computing using networks of memristors: effects of topology and heterogeneity *Nanoscale* **15** 9663–74

[197] Mallinson J B and Brown S A 2023 Time-multiplexed reservoir computing with percolating networks of nanoparticles *2023 Int. Joint Conf. on Neural Networks (IJCNN)* (IEEE) pp 1–7

[198] Mallinson J B, Steel J K, Heywood Z E, Studholme S J, Bones P J and Brown S A 2024 Experimental demonstration of reservoir computing with self-assembled percolating networks of nanoparticles *Adv. Mater.* **36** 2402319

[199] Kan S, Nakajima K, Asai T and Akai-Kasaya M 2022 Physical implementation of reservoir computing through electrochemical reaction *Adv. Sci.* **9** 2104076

[200] Cucchi M *et al* 2021 Reservoir computing with biocompatible organic electrochemical networks for brain-inspired biosignal classification *Sci. Adv.* **7** eabh0693

[201] Zhu R, Eshraghian J K and Kuncic Z 2023 Memristive Reservoirs Learn to Learn (arXiv:2306.12676)

[202] Feketa P, Meurer T and Kohlstedt H 2022 Structural plasticity driven by task performance leads to criticality signatures in neuromorphic oscillator networks *Sci. Rep.* **12** 15321

[203] Boedecker J, Obst O, Lizier J T, Mayer N M and Asada M 2012 Information processing in echo state networks at the edge of chaos *Theory Biosci.* **131** 205–13

[204] Metzner C and Krauss P 2022 Dynamics and information import in recurrent neural networks *Front. Comput. Neurosci.* **16** 876315

[205] Cramer B, Stöckel D, Kreft M, Wibral M, Schemmel J, Meier K and Priesemann V 2020 Control of criticality and computation in spiking neuromorphic networks with plasticity *Nat. Commun.* **11** 2853

[206] Loeffler A, Zhu R, Hochstetter J, Diaz-Alvarez A, Nakayama T, Shine J M and Kuncic Z 2021 Modularity and multitasking in neuro-memristive reservoir networks *Neuromorph. Comput. Eng.* **1** 014003

[207] Milano G, Montano K and Ricciardi C 2023 In materia implementation strategies of physical reservoir computing with memristive nanonetworks *J. Appl. Phys.* **56** 084005

[208] Diederich N, Bartsch T, Kohlstedt H and Ziegler M 2018 A memristive plasticity model of voltage-based STDP suitable for recurrent bidirectional neural networks in the hippocampus *Sci. Rep.* **8** 9367

[209] Paroli B, Martini G, Potenza M A C, Siano M, Mirigliano M and Milani P 2023 Solving classification tasks by a receptron based on nonlinear optical speckle fields *Neural Netw.* **166** 634–44

[210] Martini G, Mirigliano M, Paroli B and Milani P 2022 The receptron: a device for the implementation of information processing systems based on complex nanostructured systems *Jpn. J. Appl. Phys.* **61** SM0801

[211] Hoffmann G W 1986 A neural network model based on the analogy with the immune system *J. Theor. Biol.* **122** 33–67

[212] Bergstra J and Bengio Y Random search for hyper-parameter optimization

[213] Cai F, Correll J M, Lee S H, Lim Y, Bothra V, Zhang Z, Flynn M P and Lu W D 2019 A fully integrated reprogrammable memristor–CMOS system for efficient multiply–accumulate operations *Nat. Electron.* **2** 290–9

[214] Kim H, Mahmoodi M R, Nili H and Strukov D B 2021 4K-memristor analog-grade passive crossbar circuit *Nat. Commun.* **12** 5198

[215] Migliorini L, Villa S M, Santaniello T and Milani P 2022 Nanomaterials and printing techniques for 2D and 3D soft electronics *Nano Futures* **6** 032001

[216] Zhang G Q and Roosmalen A (eds) 2009 *More than Moore: Creating High Value Micro/Nanoelectronics Systems* (Springer)

[217] Sacchetto D, De Micheli G and Leblebici Y 2012 Multiterminal memristive nanowire devices for logic and memory applications: a review *Proc. IEEE* **100** 2008–20

[218] Decarli M, Lorenzelli L, Guarnieri V, Barborini E, Vinati S, Ducati C and Milani P 2009 Integration of a technique for the deposition of nanostructured films with MEMS-based microfabrication technologies: application to micro gas sensors *Microelectron. Eng.* **86** 1247–9

[219] Snider G S and Williams R S 2007 Nano/CMOS architectures using a field-programmable nanowire interconnect *Nanotechnology* **18** 035204

[220] Snider G S 2007 Self-organized computation with unreliable, memristive nanodevices *Nanotechnology* **18** 365202

[221] Caruso F, Bellacicca A and Milani P 2016 High-throughput shadow mask printing of passive electrical components on paper by supersonic cluster beam deposition *Appl. Phys. Lett.* **108** 163501

[222] Milani P and Bettini L G 2017 Nano- and micromanufacturing with nanoparticles produced in the gas phase: an emerging tool for functional and length-scale integration *Gas-Phase Synthesis of Nanoparticles* ed Y Huttel (Wiley) pp 365–85